Characterization and *in vivo* Tracking of transplanted Oligodendrocyte Progenitor Cells in the Injured Rat Spinal Cord

A Thesis
SUBMITTED TO THE FACULTY OF
UNIVERSITY OF MINNESOTA
BY

Rebecca Mahoney

IN PARTIAL FULFILLMENT OF THE REQUIREMENTS
FOR THE DEGREE OF
MASTER OF SCIENCE

Advisors: Dr. Ann Parr, Dr. James Dutton

December 2014

Acknowledgements

MRI scans were performed by Xiao Wang at the Center for Magnetic Resonance Research at the University of Minnesota
NMR spectra were acquired by Todd Rappe at the Minnesota NMR Center at the University of Minnesota

Abstract

A new method to track cells *in vivo* utilizes proton (^{1}H) magnetic resonance imaging (MRI) with ^{19}fluorine MRI. Cells can be labeled *ex vivo* with the ^{19}F reagent prior to transplantation and imaged with MRI to generate a signal detected by a custom made, dual-tone fluorine coil to show transplanted cell "hotspots" in the host tissue. Oligodendrocyte Progenitor Cells (OPCs) are an ideal cell population for cellular therapy in traumatic spinal cord injury due to their ability to remyelinate and support axons after injury. OPCs can be labeled with ^{19}F at a similar efficiency as other cell types, confirmed by fluorescence microscopy and NMR spectroscopy. Potential real-time, *in vivo* cellular tracking of transplanted OPCs would allow for analysis of cell migration after transplantation, comparison of functional analysis with transplanted cell numbers and location at multiple time points for each animal, and quantification of transplanted cells. Cell characterization of transplanted iPSC derived OPCs in injured rat spinal cords has been optimized, and can be translated to ^{19}F labeled cell transplants in the future. The FDA approved Cell Sense ^{19}F reagent allows for direct translation to use in humans for cell visualization and tracking that is not possible in current clinical trials for cellular therapies.

Table of Contents

List of Tables

List of Figures

Introduction

Oligodendrocyte Progenitor Cells

Oligodendrocyte Progenitor Cells (OPCs) and oligodendrocytes are an important cell lineage because of their myelinating function in the central nervous system (CNS) and therapeutic potential. The tightly compacted myelin sheath produced by oligodendrocytes is composed of lipid rich membranes wrapped around axons. This creates regions of high resistance and low capacitance, essential for efficient neuronal electrical signal conductance [1]. The distribution of voltage gated ion channels in the axons are organized by the myelin internodes to generate efficient signal conduction throughout the neuroaxis [2]. The myelin sheath also provides support to the axons and plays a critical role in maintaining axon integrity through protection during inflammatory events.

During embryogenesis in vertebrates, three distinct progenitor cell populations give rise to functionally redundant neuroepithelial precursor cells called OPCs that form all of the oligodendrocytes in the adult brain [3,4]. The majority (90%) of OPCs that populate the spinal cord are generated in the pMN domain of the ventral ventricular zone, and the remaining 10% are generated in a dorsal region of the spinal cord later in development. Olig2 positive cells in the pMN domain give rise to motor neurons and OPCs, following a neuronal/gliogenic switch, and a small subset of these cells give rise to astrocytes and ependymal cells [4–6]. Although most OPCs differentiate into mature oligodendrocytes, some OPCs persist into adulthood and aid in oligodendrocyte turnover and potentially myelin repair after minor injury in the CNS [7]. However, this is insufficient to provide sufficient functional recovery after spinal cord injury.

In response to injury and demyelination, endogenous OPCs are activated, primarily through inflammatory mediators, and begin the process of remyelination. The activated OPCs migrate to the area of damage through chemotaxis and proliferate[8]. At the site of damage, the OPCs begin to differentiate into oligodendrocytes and produce myelin to insulate the exposed

axons. Exposed axons are subject to irreversible damage and degradation. This dynamic process emphasizes the importance of OPCs in the adult CNS to act as a stem cell population, maintaining the levels of OPCs and mature oligodendrocytes (see Figure 1)[1,9]. This is necessary because the non-migratory and post-mitotic nature of mature oligodendrocytes prevents them in aiding the remyelination process [8].

Figure 1: Myelination in the Central Nervous System

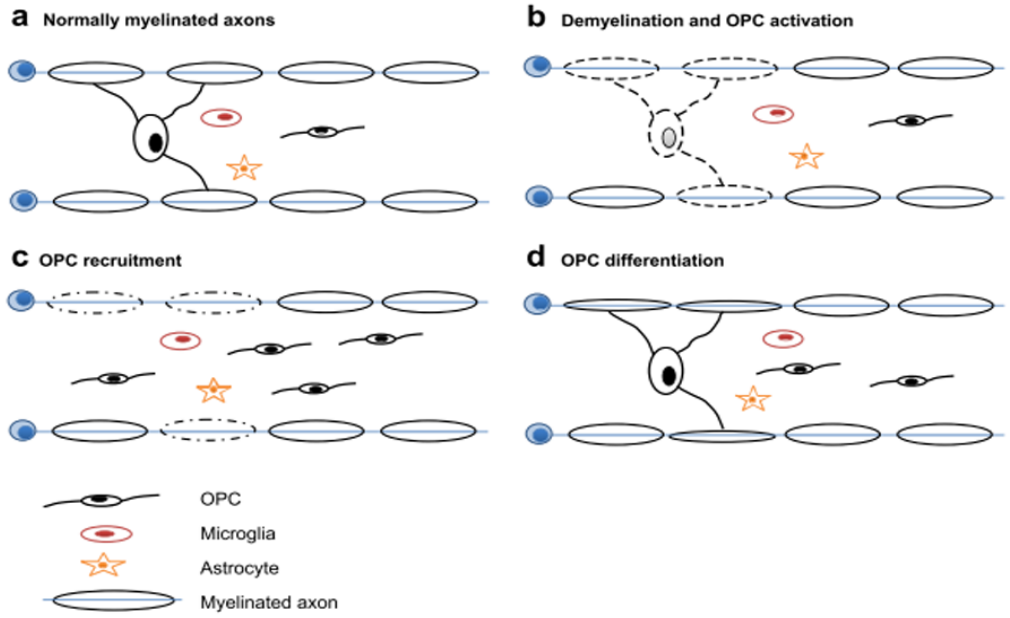

Figure 1: Myelination in the Central Nervous System. Figure adapted from Crawford et al. 2013. Under normal physiologic conditions, oligodendrocytes have produced the protective myelin sheath enveloping axons (a). After trauma due to injury or disease, oligodendrocyte death and demyelination of axons occurs (B). In response, OPCs in the adult tissue are activated and migrate to the area of demyelination through chemotaxis (C). Once in the proper location, OPCs begin to differentiate into oligodendrocytes and remyelinate the exposed axons.

Many groups are working to derive OPCs from rodent and human embryonic stem (ES) cells [10–15] and induced pluripotent stem (iPS) cells [16–18]. However, in most cases the derivation of OPCs vary in quantity and quality resulting from inconsistencies between protocols, and the

reproducibility of results needs to be established (reviewed in [9]). Additionally, these protocols are ultimately not clinically relevant as they are not translatable to Good Manufacturing Practice, a requirement for clinical use.

Oligodendrocyte Progenitor Cells and Spinal Cord Injury

The use of OPCs in the treatment of demyelinating diseases, including leukodystrophies, multiple sclerosis (MS), and spinal cord injury (SCI), has been proposed, both through activation of endogenous OPCs and transplantation of exogenous, cultured OPCs.

After traumatic SCI, there is immediate death of neurons, oligodendrocytes, astrocytes, and endothelial cells at the injury location, known as the primary injury. Death of endothelial cells results in hemorrhage, leading to vascular damage and inflammation. This is followed by spreading of secondary injury due to cell necrosis, which is worsened by macrophage and lymphocyte infiltration. Cell death and tissue loss during this phase can be attributed to ischemia, excitotoxicity of the microenvironment, edema, and inflammation. This ultimately leads to spinal cord atrophy with the presence of fluid filled cysts during the chronic phase after injury (reviewed in [19]).

A major effect of SCI is the death of oligodendrocytes at the site of injury and in distant areas from the impact site. This is thought to contribute to the loss of function following SCI. Apoptosis of distant oligodendrocytes is likely a result of an autoimmune reaction of MBP-reactive T cells infiltrating the spinal cord after injury [20]. This is supported by evidence that suppression of the adaptive immune response provides neuroprotection after SCI.

Following traumatic SCI, there is evidence for endogenous stem and progenitor population activation. Cell division and proliferation of these populations is seen as early as 24 hrs after injury. These populations give rise to new glial cells and the generation of new myelin in the injured cord [21]. However, the spontaneous remyelination seen after injury generally produces

thin myelin that is unable to compensate for the degraded myelin sheath. These findings of endogenous progenitor cell activation in the CNS indicate potential roles for these cells in therapies following SCI and CNS damage.

Due to the lack of self-regeneration and definitive treatment options following traumatic SCI, cell replacement therapies are a viable option to help restore function after traumatic SCI. In particular, the transplantation of OPCs holds great potential due to their ability to migrate and remyelinate axons at the site of injury. Several groups have investigated the use of OPCs derived from pluripotent stem cells to increase functional recovery, and have seen promising results in animal models [11,13,22–24]. Additionally, a phase 1 clinical trial was previously approved to test the safety of human embryonic stem cell (hESC) derived OPCs in patients with subacute SCI [25].

Cell Tracking in Transplantation Studies

In cell transplantation studies, the most common method of identifying transplanted cells is through post mortem analysis via immunohistochemistry (IHC). This can be done through particular staining of antigens specific to donor cells or lineage tracing of donor cells. For example, donor cells can be derived from an animal containing an eGFP reporter, such as the mouse OPCs utilized in this thesis, which can be detected in the host tissue, using fluorescence microscopy. If the donor and host cells are of different species, there are also species specific antigens, such as human Nuclear Antigen and the human cytoplasmic marker SC121 [26], to detect transplanted cells in the host tissue.

Although these methods of immunohistochemistry work well, there are many disadvantages to this form of cell tracking. For instance, the post mortem analysis limits each tissue sample to only one time point for analysis. This can present challenges for transplantation studies, especially those investigating migratory cells. If there is no initial marking of the

transplantation site, it can be challenging to accurately measure migration patterns and distances traveled *in vivo*. This type of analysis requires many animal subjects in the studies to allow for a sufficient amount of data to be collected at each time point to accurately describe cell characteristics and location over a timeline.

To account for these shortcomings, many researchers are developing methods of tracking cells *in vivo* using magnetic resonance imaging (MRI) and other imaging techniques commonly used in humans. MR imaging has advantages over other methods as it provides high-resolution images without exposing patients to potentially harmful radiation that occurs with other imaging techniques, such as Computed Tomography (CT), Positron Emission Tomography (PET), and x-ray imaging. This is especially important for patients participating in a treatment that would require regular scans, such as tracking transplanted cells.

In Vivo Cell Tracking with ^{19}F

One particular imaging technique that is gaining popularity utilizes an isotope of fluorine, ^{19}F [27]. This is a non-radioactive element that is stable in nature. ^{19}F NMR spectroscopy has been used since the 1970's to study proteins and biological materials [28]. This technology has recently expanded to utilize ^{19}F for imaging through the use of perfluorocarbon (PFC) - based cell labels. PFCs are the most biologically inert organic molecules produced and are non-toxic to cells, even at high doses [29]. Fluorocarbons do not degrade at lysosomal pH values and there are no known enzymes that metabolize the compounds, likely due to the strong, covalent C-F bond [30]. ^{19}F has many characteristics that make it ideal for MR imaging, including its non-toxic and stable nature, and its infrequency in biological materials creating low background [29]. MR imaging is accomplished utilizing the natural magnetic properties of organisms. Typically, the hydrogen nucleus is used to generate an image because of its abundance in the body. Using the strong magnetic field of the MRI scanner, the protons align uniformly in the magnetic field. By

changing the local magnetic field through a series of gradient electric coils, different tissues of the body will produce different signal intensities. Additional wave pluses at radio wave frequency cause the hydrogen nuclei to resonate and emit a signal once the radiofrequency is shut off. This signal is received and plotted to generate stacked, cross sectional images [31].

Another method utilized by labs to track cells *in vivo* with MRI is cell labeling with superparamagnetic iron oxide nanoparticles (SPIOs). SPIOs are clinically used T_2 contrast agents. These SPIOs were not designed to be intracellular labels and can only be taken up by phagocytes or the use of transfection agents is required for intracellular labeling. Recently, SPIOs have been coated with dextran or heparin (HSPIO), which allows them to enter non-phagocytic cells[32]. This labeling approach has been used by multiple groups to track transplanted stem cells *in vivo* in mouse and rat models, including studies focused on the CNS[33]. These studies have emphasized the possibility and importance of tracking transplanted cells using conditions that are clinically relevant. However, the SPIOs often look like blood on the MR image. Areas of hemorrhage make it difficult to distinguish the iron-oxide containing stem cells, providing a large obstacle in cell tracking[33].

In comparison to more commonly used metal ion- based contrasts that rely on ^{1}H-MRI imaging, ^{19}F imaging utilizes multi-nuclear MRI that will not interfere with T_2- or diffusion-weighted imaging [34]. To accomplish this, a different radiofrequency is used to detect fluorine nuclei and generate an image of fluorine signals overlaid with the corresponding ^{1}H image. For example, a study conducted by Bible et al. utilized this technique to track ^{19}F labeled human neural stem cells transplanted into a stroke model. With this reagent they were able to perform real-time imaging to confirm that the transplanted cells were injected into the correct area of the brain and did not migrate out of this area after transplantation.

Another important factor in measuring recovery after stroke injury is to observe the lesion cavity size, imaged by diffusion MRI. Diffusion MRI is a type of ^{1}H imaging that can be

affected with the use of metal oxide labeling, such as iron oxide or gadolinium, decreasing the ability to analyze stroke pathology with MRI. With the use of ^{19}F labeling agent, this group was able to visualize the transplanted human neural stem cells and make accurate measurements of the lesion cavity using multi-nuclear MRI.

^{19}F cell imaging has great implications in the field of cellular therapy. One large obstacle to FDA approval of cell therapies is the inability to track the persistence and location of transplanted cells. This technology is safe for human use and provides a platform to measure cell quantity and location *in vivo* while simultaneously tracking functional improvement [35–37].

Multiple types of PFC have been developed, however the ideal compound for imaging contains a simple NMR spectrum with a single peak. NMR spectroscopy measures the amount of fluorine nucleus spins in a strong magnetic field after exposure to an appropriate radiofrequency. ^{19}F NMR spectroscopy is a useful tool in quantifying ^{19}F. Magnetically nonequivalent fluorine molecules will generate multiple peaks on the spectrum. A single peak, representing magnetically equivalent fluorine molecules, is ideal to generate a maximized signal intensity for the PFC. The particular FDA approved nanoemulsion ^{19}F compound, Cell Sense, generated by the company Celsense, is a linear perfluoropolyether (PFPE) polymer. This PFPE is an ideal ^{19}F compound because of its single NMR resonance peak and small T_1/T_2 ratio, providing an intense signal with minimal background with MRI. The linear structure of this compound allows it to be conjugated to other compounds, such as fluorescent dyes, for increased functionality [29]. This also gives the PFPE self-delivering abilities that allow the compound to enter the cell without the need for transfection, making the compound easy and safe to use [38]. This is in contrast to the metal ion labeling techniques that may require transfection to label non-phagocytic cells.

Cell Sense has been used to label a variety of different cell types, including T cells, dendritic cells, hematopoietic stem cells, neural stem cells, and mesenchymal stem cells [37,39–41]. A phase I clinical trial is currently ongoing using Cell Sense to label therapeutic cells *ex vivo*. The

study is investigating an immunotherapeutic dendritic cell vaccine to treat stage-4 colorectal cancer [35]. The goal of the study is to show the safety of both the dendritic cell vaccine and the Cell Sense reagent. The vaccine was injected into peripheral tissue, with the intention that the cells would migrate to the lymph node. In the three participating patients, there is a decreased signal in the area of injection 24 hrs following transplantation, indicating that roughly half of the injected cells were no longer at the site of injection and had potentially migrated to the lymph node or other tissues.

The versatility of PFCs is emphasized in this clinical trial and previous studies. ^{19}F is an easy to use cell label to visualize either transplanted cells that migrate after transplantation in a short term imaging study, or for prolonged imaging of transplanted cells that remain stationary after injection, as in the models of stroke [42,43]. The intensity of the signal produced by the ^{19}F can be used to quantify the number of labeled cells, which is important for transplantation studies but can prove to be challenging using conventional IHC methods. This is especially true in human clinical trials, where quantification of transplanted cells is important for evaluation of safety and efficacy but is currently challenging. Additionally, the short term imaging approach can confirm proper transplantation, both in cell number and location, relatively soon after the procedure. This is especially useful for difficult procedures that often result in graft failures, such as cell therapies for spinal cord injury [26]. Without *in vivo* imaging, it is impossible to know if the therapeutic cells were properly delivered until the tissue is harvested and processed post mortem. This is problematic for evaluating efficacy of cell therapies in clinical trials and can result in an increased number of animals used in pre-clinical studies as well as increased costs and duration of the study.

In Vivo Cell Tracking of Transplanted Oligodendrocyte Progenitor Cells

Despite the range of cell types that have been studied with PFC tracking, no studies have been conducted in spinal cords or with OPCs. The studies done on human neural stem cells indicates that cells in the CNS can be labeled and imaged using these techniques. However, most of the studies that have been conducted are on either highly migratory cells, for example dendritic cells and T lymphocytes, or stationary cells, such as neural stem cells in a scaffold [34,36,40]. OPCs are an intermediate to those cell types; OPCs are able to migrate through the spinal cord to the site of injury, however this is a smaller environment than the hematopoietic or lymphatic systems. Thus, it is possible that the migration of OPCs could be visualized at early time points after transplantation, in addition to observing their long term location in the spinal cord. Using ^{19}F tracking would allow for the confirmation that transplanted OPCs can migrate to the injury site, while observing any pathological improvements in the spinal cord with MRI. Of the ongoing clinical trials using cellular therapies to treat SCI, it is difficult to precisely determine if the functional improvements are a result of the transplanted cells or if they are a result of another phenomenon. *in vivo* tracking would shed light on these important questions.

The purpose of this study is to validate the safety and non-toxicity of ^{19}F Cell Sense reagent in iPS cell derived OPCs and to determine if this is a viable method of *in vivo* cell tracking of transplanted OPCs in injured rat spinal cords (**Part A**). *ex vivo* labeling analysis is confirmed with NMR spectroscopy and viability testing. Effectiveness of *in vivo* tracking will be confirmed with normal histological, post mortem analysis. Therefore it is important to optimize cell tracking and characterization using immunohistochemistry in OPC transplantation experiments without the ^{19}F Cell Sense reagent (**Part B**). If *in vivo* tracking of iPS cell derived OPCs is possible in the injured rat spinal cord, this would provide more insight to the role of transplanted OPCs in injured cords. This potential application is directly translatable to human

use in the current and future clinical trials transplanting OPCs in injured spinal cords given the safety and FDA approval of the ^{19}F Cell Sense reagent.

Materials and Methods

Part A: Cell Labeling and Tracking with ^{19}Fluorine

Mouse Oligodendrocyte Progenitor Cells

Mouse iPS cell derived OPCs have been previously generated in the Parr lab from Oct4:CreER mGmT iPS cells [44]. These cells express transmembrane eGFP. The cell population was profiled using immunocytochemistry and quantitative PCR (qRT-PCR), confirming a heterogeneous population containing a majority of OPCs and small percentage of neural and astroglial markers.

Mouse Cell Culture

Frozen mOPCs were provided in culture or thawed at room temperature. After removing the cells, the Cryovial® was washed two times with mOPC media, containing the base media Dulbecco's Modified Eagle Medium/ Nutrient Mixture F-12 (DMEM/F-12) (Gibco® by Life Technologies), 2% B27 Supplement (Gibco® by Life Technologies), 1% N2 Supplement (Gibco® by Life Technologies), 1% Penicillin/Streptomycin (Corning Cellgro), 0.001% Recombinant Human Sonic Hedgehog (Shh) (C24II) N-Terminus (100 µg/mL) (R and D Systems), 0.0002% Recombinant Human FGF (146 aa) Basic (100µg/mL) (R and D Systems), and 0.0002% PDGF-AA Human (100 µg/mL) (Sigma-Aldrich). This mOPC media was optimized for the appropriate combination and balance of growth factors previously by the Parr lab. After cell removal and washing, the freezing media, 10% DMSO in mOPC media, was diluted 1 to 10 with growth media in a 15 mL conical and the suspension was centrifuged at 1000 RPM for 5 minutes. The supernatant was removed, and the pellet was resuspended in 1 mL of mOPC media using a p1000 pipettor. An additional 5 mL of mOPC media was added to the cells, and 1 mL of the cellular solution was added to each well of a prepared 6 well plate. The 6 well pate was prepared by coating each well with 1 mL poly-ornithine 50 µg/mL (Sigma-Aldrich) for

1 hr, up to 24 hours. The poly-ornithine was removed, and each well was washed twice with 1 mL of sterile water and then with 1 mL of Fibronectin (50 µg/mL) (Sigma-Aldrich). Finally, each well received 1 mL of mOPC media before adding the cellular suspension. The cells were evenly distributed throughout the plate and incubated at 37° C, 5% CO_2. The following day the media was changed, followed by subsequent media changes every 2 days while the cells were maintained in culture. When cells became 90% confluent, typically after 3 days in culture, the cells were passed.

During passaging, the media was removed from the wells. Each well was washed with 1 mL sterile PBS and 1 mL of accutase (Millipore) was added to each well to enzymatically detach the cells from the plate. The cells were incubated with accutase for 5-10 minutes at room temperature, until the cells were round and detached from the plate on their own. The cell suspension was collected in an appropriate conical, most commonly three 15 mL conicals, with 2 wells per conical. Each well was rinsed twice with 1 mL mOPC media each, adding the solution to the respective conical. The conicals were then filled with media to properly dilute the accutase and prevent cell damage or death and the cells were pelleted. The supernatant was aspirated and each cell pellet was resuspended in 1 mL of mOPC media. An additional 5 mL of mOPC media was added, and each conical was evenly distributed to one previously prepared 6 well plate for a 1 to 3 passage. The media was changed on the following day, with media changes occurring every other day after.

Human Cell Culture

Human Lung Fibroblasts (HLF) were used in early experiments to test labeling efficiencies and viability after ^{19}F labeling. The cells were provided in live culture and were maintained in HLF media provided.

Human iPSC derived OPCs (hOPCs) were provided in live culture for ^{19}F labeling to ensure safe uptake the ^{19}F reagent. hOPCs were maintained on Laminin (20 µg/mL, Life Technologies) coated plates in provided hOPC medium, N2/B27 Basal media supplemented with triiodothyronine (40 ng/mL), Insulin-like Growth Factor-1, Neurotropin-3, Platelet-Derived Growth Factor AA (20 ng/mL), and Epidermal Growth Factor.

In all cell cultures, the cells were routinely monitored for signs of contamination.

Cell Viability

Cell viability was measured based on morphology and Trypan Blue staining. Cell morphology was routinely observed using microscopy. During cell passaging or harvesting, a small aliquot was removed for quantification and viability testing by diluting the aliquot with Trypan Blue. The cells were counted using a hemocytometer and the total cell counts and percent of blue, or dead cells, was recorded.

Labeling Human Lung Fibroblasts and Oligodendrocyte Progenitor Cells with ^{19}F

The cell labeling experiments were done to determine the optimal loading of fluorine in HLFs and OPCs with the greatest cell survival and intracellular ^{19}F concentration.

The company Celsense generated a perfluorocarbon (PFC) cell labeling product optimized for *ex vivo* cell labeling for transplantation studies called Cell Sense (CS-ATM). This is a linear perfluoropolyether (PFPE) polymer containing >20 ^{19}F molecules [38]. The linear nature of this compound allows it to be directly conjugated to a fluorescent dye, here the red BODIPy-TR dye was used. The linear PFPE is formulated into a nanoemulsion with an FDA approved copolymer, F68, and a polyamine containing both primary and secondary amine groups, essential for cellular uptake [38]. This nanoemulsion compound is called CS-ATM DM Red, hereafter referred to as CS-ATM.

Figure 2: The CS-ATM DM Red ^{19}F compound

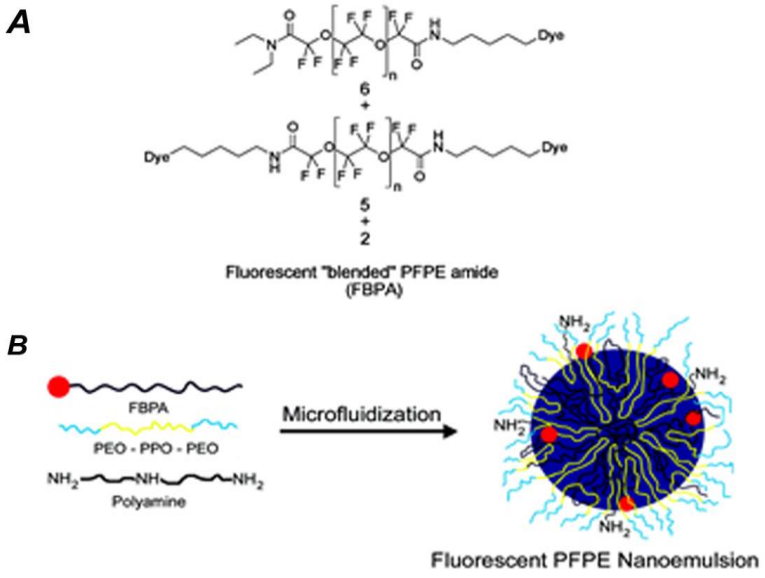

Figure 2: The CS-ATM DM Red ^{19}F Compound. Figure adapted from Janjic et al. The PFPE polymer with ^{19}F molecules is conjugated to a fluorescent dye (BODIPy-TR) for dual functionality, with the end result designated as FBPA here (A). The FBPA undergoes microfluidization with F68, a compound with hydrophobic polypropylenoxie (PPO) and hydrophilic polyethylene oxide (PEO) groups, and a polyamine to generate the nanoemulsion used for cell labeling.

In initial experiments, HLF cells were used to determine labelling protocols and toxicity of CS-ATM. HLF cells were provided live in culture were incubated in CS-ATM for 24 hrs. Ten different concentrations of CS-ATM were used, 2.5, 5, 7, 10, 12.5, 15, 17, 20, 25, and 30 mg/mL, diluted with HLF media. Two negative controls with only HLF media were included. After the 24 hr incubation period, the cells were washed several times with sterile phosphate buffered solution (PBS) and kept in culture for two additional days. At the end of this time the cells were analyzed for fluorine uptake and viability.

Similar labeling experiments were repeated with mOPCs. The cells were incubated in culture for 24 hrs with CS-ATM. CS-ATM was diluted in mOPC media to achieve the concentrations of 2.5, 3, 5, 7.5, and 10 mg/mL. In all experiments at least one negative control was included with no CS-ATM in the media. To increase cellular uptake of fluorine, 10% Human Serum Albumin (1mg/mL) (Calbiotech) was added to the CS-ATM media [34]. After the 24 hr incubation period, the mOPCs were washed and analyzed. After ^{19}F labeling, the cells maintained in culture for up to 9 days. The cells were typically analyzed shortly after removal of the CS-ATM compound to prevent signal dilution from concurrent cell divisions after ^{19}F reagent removal.

hOPC labeling was done by incubating CS-ATM at 4 mg/mL diluted in M1 media for 24 hrs. After incubation the cells were washed repeatedly with PBS and fixed with Formalin (Fisher Scientific, 1:10 dilution).

Fluorescence Labeling Analysis

Fluorescence was measured using fluorescence microscopy on the Leica CTR HS microscope and Leica Application Suite Advanced Fluorescence 3.1.0 software. Post image analysis was completed with ImageJ.

For *in vitro* analysis, the cells were fixed on the plate or in suspension using Formalin. The cells were then counter stained with Dapi, diluted 1 to 1000 in PBS with .1% Tween (PBS-T), incubated for 2-5 minutes, and then washed with PBS. Fluorescence microscopy was used to visualize the cells. Overlaid images were obtained in the Red, Green, and Blue channels to confirm normal cell morphology and CS-ATM uptake by eGFP positive cells, designated by red fluorescence. The exposures and intensity for each channel were held constant for each experimental trial.

The images of red fluorescence were used to determine Relative Fluorescent Units (RFU) and quantify CS-ATM uptake. Overlaid images in the red and blue channel were used to determine the amount of CS-ATM (red) per cells, designated by Dapi staining. The quantification was done using the Color Histogram plugin on image processing software, ImageJ. This plugin calculated the total amount of red pixels and total amount blue pixels in a selected area of the image. The red pixel value was divided by the blue pixel value to determine the amount of red per cell for each image. For each sample, 5 random fields were analyzed. The average of the 5 fields was used for the final analysis.

The CS-ATM nanoemulsion contains red fluorescent dyes directly conjugated to the ^{19}F. Because of this, the relative amounts of fluorine per cell can be estimated by the fluorescence values in order to derive a relationship between the cellular ^{19}F labeling for different concentrations of CS-ATM.

Nuclear Magnetic Resonance Spectroscopy for Quantification of ^{19}F

For an accurate quantification of fluorine content per cell, high-resolution nuclear magnetic resonance (NMR) spectroscopy was used. Samples were prepared by labelling HLF cells and mOPCs as described with CS-ATM. After 24 hrs of labelling, the cells were washed with PBS, harvested using accutase, and counted. According to the cell counts, appropriate aliquots were removed to obtain a sample of 100,000 cells. Each sample was spun down to obtain a dry cell pellet. The cell pellets were resuspended in a NMR lysis buffer, according to the manufacturer's instructions. The NMR lysis buffer contains 25% deuterium oxide (D_2O) at >95% purity (Sigma-Aldrich), 25% 2% Trion X-100 (Sigma-Aldrich), and 50% .01% Trifluoroacetic acid (TFA). The presence of D_2O allows for the hydrogen on the –OH group on the acid to be replaced with deuterium, which prevents hydrogen bounding between molecules to give a clear NMR spectrum. Triton X-100 was used to lyse the cells by permeablizing the membrane,

allowing the intracellular components (^{19}F) to be analyzed. TFA provided and internal reference used to calibrate the fluorine NMR spectrum.

Prepared samples of known cell concentrations were delivered to the University of Minnesota NMR center. A 600 MHz spectrometer with the AutoX Dual BB PFG probe was used for all fluorine NMR analysis. Both the CS-ATM and TFA reference appear as a single, narrow resonance peak, at -91 and -76 ppm, respectively. After data acquisition, the integrated area under each peak was calculated and used to determine the amount of fluorine atoms per cell for each sample. The amount of fluorine per cell (F/C) was calculated with the formula provided by Celsense:

$$(F/C) = \frac{3 I_s M_r N_a}{I_r N_c}$$

I_s = integrated area of major peak of the cell pellet
M_r = moles of TFA reference (Note: three ^{19}F per TFA molecule already reflected in equation, 1.75×10^{-6} moles if above quantities are used)
N_a = Avogadro's number
I_r = integrated area under TFA reference peak
N_c = number of cells in pellet

The calculated values of fluorine molecules per cell were used in correspondence with MRI phantom experiments to determine the number of cells necessary to generate a signal with enough intensity to be visualized using the MRI technologies.

Magnetic Resonance Imaging of ^{19}F

Imaging was performed at the Center for Magnetic Resonance Research (CMRR) at the University of Minnesota. The Varian 16.4T MRI scanner was used for all imaging experiments.

Initial magnetic resonance imaging (MRI) experiments were done to validate the fluorine detection by the custom made dual-tone coil and to determine the amount of ^{19}F molecules

needed for visualization. The first cell-free "phantom" experiment consisted of six 0.2 mL PCR tubes filled with equal amounts of CS-ATM, 10 µL diluted to 200 µL with PBS, place evenly in a 2 cm diameter circle in a custom made foam container. This phantom was used to ensure a uniform magnetic field throughout the coil.

The second cell-free phantom experiment was used to identify the range of fluorine needed to produce a clear image. A similar custom made foam apparatus was used, containing six PCR tubes with different amounts of CS-ATM, 0.1, 0.5, 1, 5 and 10 µL. This experiment was used to determine the lower limit of fluorine needed for signal detection. These amounts were used because of the known positive control (10 µL) to generate a signal, and smaller, biologically relevant amounts.

The third phantom experiment was used to observe ^{19}F signal detection in cells. Four cells samples containing 300,000, 600,000, 1 million, and 1.5 million cells were labeled with 5 mg/mL. This concentration of CS-ATM was used based on NMR fluorine quantification in mOPCs and the cell numbers were calculated from the second MRI phantom results. One negative control with PBS only and one positive with 0.5 µL CS-ATM in PBS were included and all 6 samples were placed in the custom foam apparatus.

Part B: Characterization of Transplanted Oligodendrocyte Progenitor Cells in the Injured Rat Spinal Cord

Cell Characterization after Transplantation into Injured Rat Spinal Cords

A short term study was conducted to observe and characterize iPS cell derived OPCs after transplantation into an injured rat spinal cord. This study was done to validate the use and safety of OPCs in the spinal cord, as well as track and characterize OPCs after transplantation, without ^{19}F labeling.

Athymic nude rats received 200 kD contusion injuries, followed by OPC transplantation 9 days post injury (DPI). Each rat received four injections, two rostral and two caudal to the injury site on the right and left sides of the cord. A total of 300,000 cells were transplanted into each rat, with 2.5 µL of cell suspension per microinjection. Eight rats received mOPC transplants, 2 rats were injected with media only controls, and 10 rats received hOPC transplants. After 1 day, 1 week, or 1 month the spinal cord from each rat was harvested and fixed.

The tissues were frozen in a freezing media, optimal cutting temperature (OCT) embedding media (Fischer Healthcare Tissue Plus®). Each spinal cord was completely embedded in OCT in a cryomold. The block was frozen in dry ice and stored at -80°C.

All tissues were processed as frozen sections, obtained using the Leica CM 3050S cryostat. The CryoJane® tape transfer system (Leica Biosystems) was used for sectioning. The slides were mounted on CSFA (Leica Biosystems) adhesive slides, placed in a slide rack, and stored at -80° C.

Immunohistochemistry

Frozen tissue sections were analyzed using immunohistochemistry to detect and characterize transplanted iPS cell derived OPCs in the injured rat spinal cord.

Frozen sections from -80° C were brought to room temperature and warmed to 37°C to melt the surrounding OCT and further adhere the tissue sections to the slide. The slides were then washed in PBS to rehydrate the tissue. A Dako barrier pen was used to create a hydrophobic barrier around each section to keep liquids tightly on each section. The tissue was permeablized with PBS + 0.1% Triton X-100 to enable antibody entry into the cells, followed by blocking in PBS + 1% Horse Serum (1mg/mL, Jackson ImmunoResearch) to prevent non-specific antigen binding. The tissue was then incubated overnight with primary antibodies diluted in an incubation buffer, 1% Bovine Serum Albumin (BSA) (Sigma-Aldrich), 1% normal donkey serum (Jackson

ImmunoResearch), 0.3% Triton x-100, and 0.01% sodium azide (Fluka Biochemika). BSA and donkey serum are included for additional blocking to prevent non-specific binding, Triton X-100 allows antibody entry into cells, and sodium azide works to preserve antibody binding. For a complete list of antibodies used Table 1.

On the following day, the sections were washed and incubated with secondary antibody diluted in incubation buffer. The slides were washed and then stained with Dapi (1:1000) for visualization of the nuclei. Immunofluorescence was analyzed using fluorescent microscopy and post image analysis was done using Adobe Photoshop and ImageJ. Positive and negative controls were obtained for each antibody used. Positive controls were performed on control CNS tissue without cell transplants. Sections receiving only the secondary antibody were used as negative controls.

Table 1: Primary and Secondary Antibody List

OPC Primary Antibodies					
Antigen	**Host**	**Dilution**	**Staining**	**Company**	**Catalog Number**
SC121	Mouse	1:500	Cytoplasmic	Stem Cell Proven	AB-121-U-050
MBP	Rat	1:250	Structural	Abcam	ab7349
Olig 2	Rabbit	1:250	Nuclear	Millipore	AB9610
Pax 6	Mouse	1:25	Nuclear	DHSB	N/A
Beta III Tubulin	Mouse	1:1000	Structural	Millipore	AB9354
Ki67 (SP6)	Rabbit	1:500	Nuclear	Abcam	ab1667
APC	Mouse	1:200	Nuclear	Calbiochem	OP80
GFAP	Mouse	1:500	Structural	Milipore	MAB360
NF200	Mouse	1:250	Structural	N/A	N/A

Secondary Antibodies				
Host	**Raised Against**	**Emission Wavelength**	**Company**	**Catalog Number**
Donkey	Mouse	555	Life Technologies	A3170
Donkey	Rabbit	555	Life Technologies	A31572
Donkey	Rat	555	Alexa Fluor	A21434

Table 1: Primary and Secondary Antibody List. Descriptions of each antibody used in this thesis is provided.

Results

Part A: Cell Labeling and Tracking with ^{19}Fluorine

Labeling HLF cells with ^{19}F

Initial *in vitro* cell labelling experiments were performed using human lung fibroblasts (HLF). Toxicity and cell viability were determined after labelling with increasing amounts of ^{19}F Celsense reagent. The concentrations used were 2.5, 5, 7, 10, 12.5, 15, 17, 20, 25, and 30 mg/mL of ^{19}F Cell Sense reagent, with two negative controls lacking fluorine (Figure 3 A-F). The cells were treated with the ^{19}F Cell Sense reagent diluted in HLF media for 24 hours, followed by washing to remove the reagent from the media and additional culture for 2 days before analysis. The amount of time for labeling (24 hours) was not used as a variable based on previous findings suggesting that 24 hours is optimal for highest ^{19}F concentrations and minimal cell toxicity[34].

Confirming ^{19}F uptake and viability of ^{19}F labeled Cells

Fluorine uptake was confirmed by fluorescent microscopy, utilizing the red fluorescent dye conjugated to the reagent (Figure 3A-F). There was a visible increase in red fluorescence, however this was not quantified. Viability testing using Trypan blue determined the cell survival in increasing ^{19}F reagent concentrations (Figure 3G-H). In conditions without reagent, the cell viability ranged from 95%-100% (Figure 3G). In the two highest concentrations, 25 and 30 mg/mL, the cell death increased to 13% (Figure 3H). During analysis, cells were persistently growing, indicating that the Cell Sense reagent does not terminate cell growth. Previous publications have indicated that ^{19}F CS-ATM labeling concentrations between 2-5 mg/mL provide an optimal balance between cell labeling and cell death [34,40,42]. In our study with HLF cells this concentration results in 95% cell viability. These viability values indicate that CS-ATM can be used in HLF cells with minimal effects on cell death and proliferation.

Previous studies have indicated that the presence of Human serum albumin (HSA) in the culture medium can increase ^{19}F reagent uptake in human cells *in vitro* [34]. Fluorescence analysis revealed increased fluorescence in labeled cells with HSA present in the media compared to cells loaded with the same concentration of CS-ATM without HSA (Data not shown).

Figure 3: CS-ATM Labeled HLF Cells and Viability

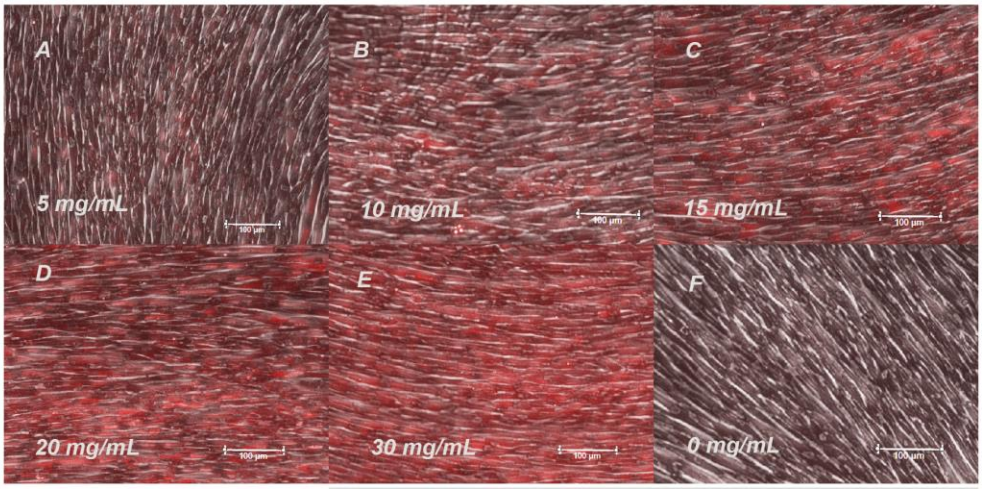

G

HLF Viability	
Concentration of CS-ATM (mg/mL)	Cell Death (%)
0	0
0	5.45
10	7.69
20	10.48
30	13.59

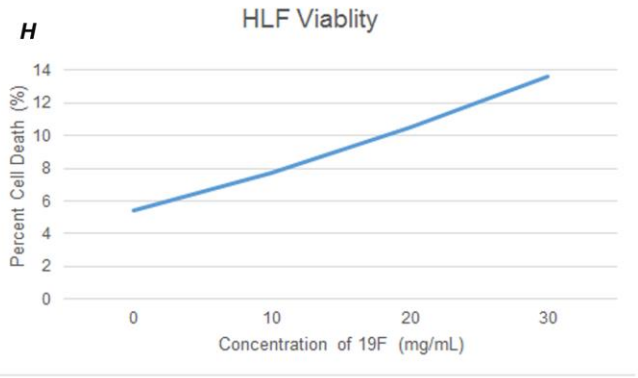

Figure 3: CS-ATM Labeled HLF Cells and Viability. (A-F) HLFs labeled with CS-ATM DM Red visualized using fluorescence and phase microscopy; 5 mg/mL (A), 10 mg/mL (B), 15 mg/mL (C), 20 mg/mL (D), 30 mg/mL (E), and a negative control (F). Scale bars all indicate 100 µm. Cell viability was determined by calculating cell death observed by Trypan Blue staining. The percent of cell death is shown as a table (G) and graphed (H).

Quantification of ^{19}F in HLF Cells Using Nuclear Magnetic Resonance Spectroscopy

Nuclear Magnetic Resonance (NMR) spectroscopy was used to accurately quantify the fluorine content of ^{19}F labeled cells.

NMR analysis with HLF cells was performed to establish a protocol for preparing cells for ^{19}F NMR detection and to determine the effect of different CS-ATM labeling concentrations and HSA on fluorine uptake. HLF cells were incubated with CS-ATM at 3 mg/mL, 3 mg/mL with 10% HSA, 5 mg/mL, and 5 mg/mL HSA. In addition, two negative controls were used, one with HLF media only and the other with 10% HSA in HLF media. On the day of NMR analysis, the cells incubated with 5 mg/mL and 10% HSA did not survive from unknown cell toxicity and were excluded from the experiment. From the remaining conditions, samples of 100,000 cells were brought to the University of Minnesota NMR facility for data acquisition (Figure 4 A-C). The results revealed that the samples labeled with 3 mg/mL, 3 mg/mL + 10% HSA, and 5 mg/mL contained fluorine in the range of 10^{11} ^{19}F molecules per cell, which is within the typical range (10^{11}- 10^{13} F molecules per cell) according to the manufacturer. The 3 mg/mL + HSA and 5 mg/mL samples had similar ^{19}F content with 6.24 x 10^{11} and 6.7 x 10^{11} ^{19}F molecules per cell (Table 1, Figure 4D). The 3 mg/mL sample was lower in fluorine content with 1.84 x 10^{11} ^{19}F molecules per cell (Table 1, Figure 4D). Overall, these results indicated that NMR detection can be used to provide an accurate calculation of ^{19}F content per cell and that the labeling performed provides fluorine uptake consistent with previous reports and the manufacturer's findings.

Figure 4: ^{19}F Quantification in HLF Cells using NMR

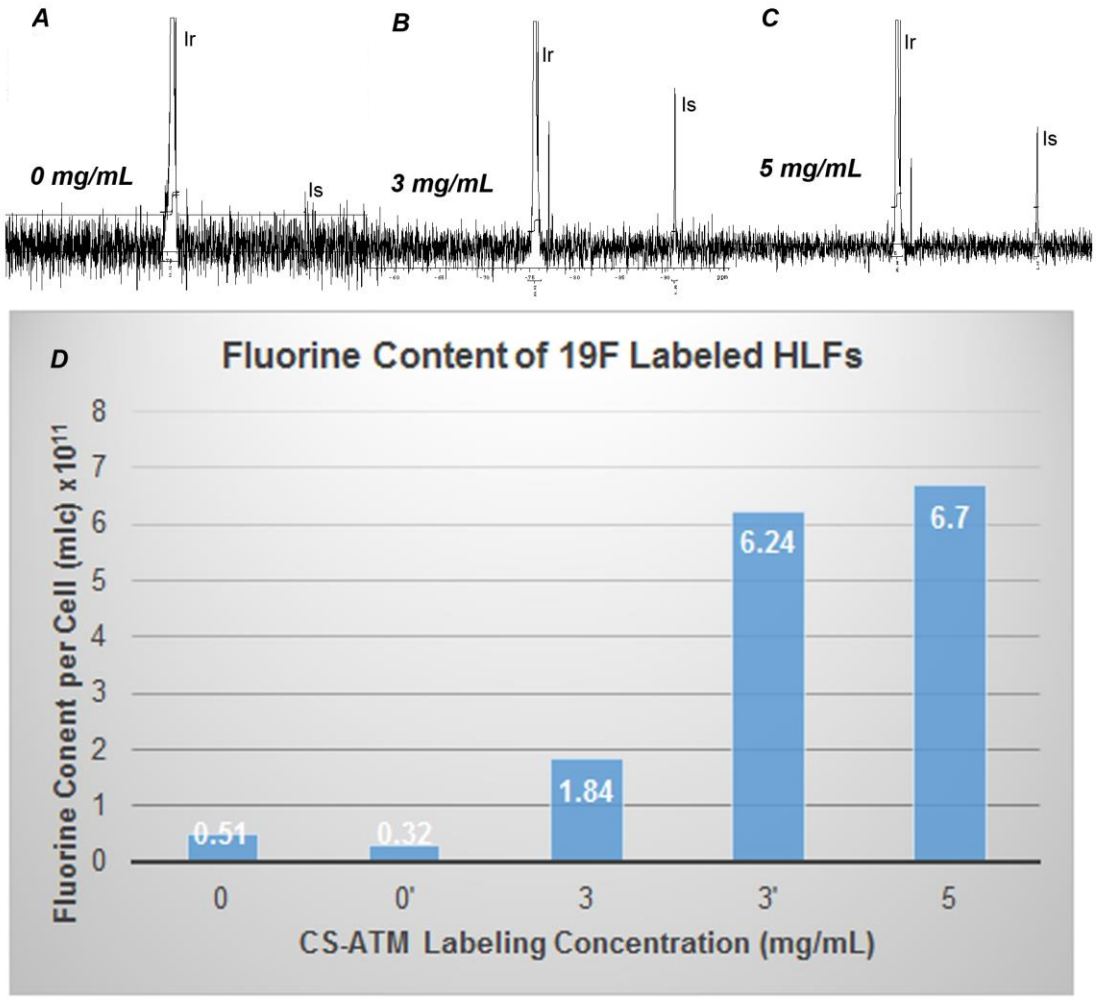

Figure 4: ^{19}F Quantification in HLF cells using NMR. Cell samples labeled with CS-ATM at different concentrations were analyzed with NMR spectroscopy. (A-C) Example spectrums obtained from NMR are provided for the negative control (A), 3 mg/mL with 10% HSA (B), and 5 mg/mL (C) labeling concentrations. On the spectrums, Ir designates the TFA reference peak at -91 ppm and Is designates the Cell Sense reagent peak at -76 ppm. The spectrums were used to calculate the amount of fluorine molecules per cell, shown in D. The X axis represents the labeling concentration, where the 3' indicates 3 mg/mL with 10% HSA and the Y axis is the amount of fluorine per cell. The numbers indicated on the graph are x10^{11}.

Labeling mouse iPSC-derived OPCs with ^{19}F

miPS cell derived OPCs were labeled with the ^{19}F CS-ATM reagent to determine conditions for optimal cell labeling with minimal cell death. mOPCs were incubated overnight with 2.5, 5, 7, and 10 mg/mL ^{19}F Cell Sense reagent diluted in mOPC media, followed by a 24 hour wash period. Fluorine uptake was confirmed using fluorescent microscopy (Figure 5A-D).

Quantification of ^{19}F labeling in OPCs using Relative Fluorescence

The ^{19}F labeling in OPCs can be estimated by directly observing the fluorescence of the BODIPy-TR conjugated to CS-ATM. This compares the efficiency of labeling or the amount of fluorine present between different experimental groups.

Images of labeled and unlabeled mOPCs were obtained by fluorescent microscopy using the same imaging parameters for each condition. The total fluorescence detected in the red channel (Figure 5 A-D) was converted to Relative Fluorescent Units (RFU) using image analysis software and is presented as the amount of fluorescence per cell for each labeling concentration (Figure 5E). The RFU increased with increasing CS-ATM concentrations with a linear trend. CS-ATM labeled cells were maintained in culture for up to 9 days and red fluorescence was still detectable after this time, although the total fluorescence appeared to decreased from the 2 day analysis time point by visualization.

Cell viability of ^{19}F labeled miPSC derived OPCs

Aliquots of ^{19}F labeled OPCs from each labeling condition were assessed for viability after fluorine uptake using Trypan Blue. Cell survival of at least 95% was determined for each condition (Figure 5F), consistent with our previous results using HLF cells.

Figure 5: CS-ATM Labeled mOPCs and Relative Fluorescence

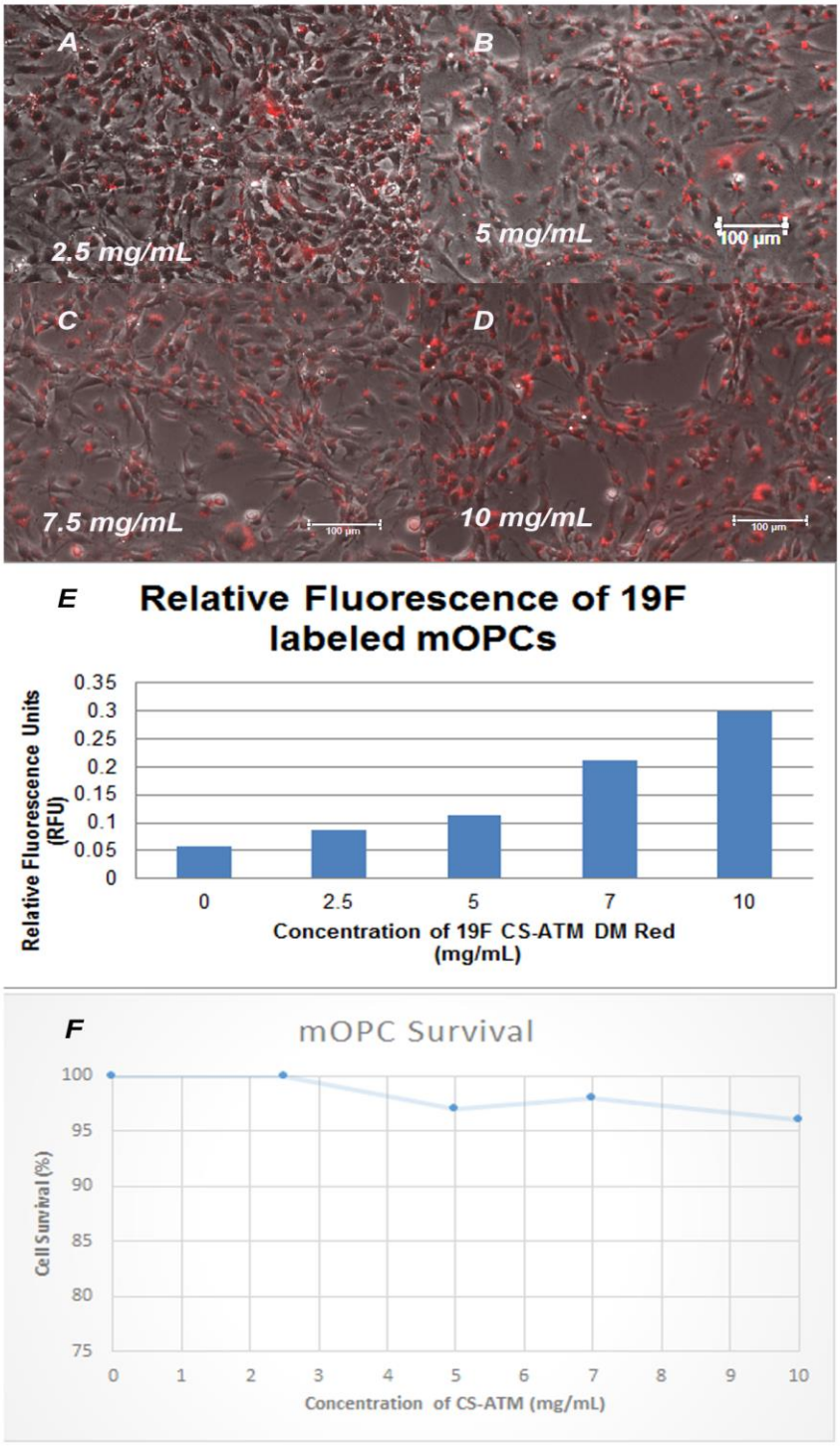

Figure 5: CS-ATM Labeled mOPCs and Relative Fluorescence. (A-D) mOPCs labeled with CS-ATM DM Red at different labeling concentrations visualized using fluorescence microscopy overlaid with phase images, with 2.5 mg/mL (A), 5 mg/mL (B), 7.5 mg/mL (C), and 10 mg/mL (D) of Cell Sense reagent. Scale bars are all 100 µm. Quantification of fluorescence as Relative Fluorescent Units (RFU) is shown in E. The X axis represents the labeling concentration of CS-ATM and the Y axis is the average RFU per sample. The percent of cell survival after labeling is also shown for each labeling concentration (F).

NMR analysis of ^{19}F labeling in miPSC-derived OPCs

NMR analysis was completed to accurately quantify the amount of fluorine uptake in mOPCs.

Two samples of mOPCs incubated with 5 mg/mL, 7.5 mg/mL, and 10 mg/mL each underwent NMR spectroscopy (Figure 6E-H). The higher incubation concentrations of CS-ATM were used in an attempt to maximize the cellular fluorine content and identify the most effective labeling concentration. The amount of ^{19}F per cell was determined for each sample and revealed similar concentrations of fluorine per cell in the range of 6-7 x 10^{11} ^{19}F molecules per cell (Table 1, Figure 6F). These concentrations are similar to but slightly lower than the HLF results for 5 mg/mL (Table 1).

Based on the NMR results, the optimal ^{19}F labeling concentration for mOPCs was determined to be 5 mg/mL and was used as the incubation concentration for the remainder of experiments. Almost the maximum fluorine uptake detected was achieved with 5 mg/mL, with only slight increases in ^{19}F molecules per cell detected with higher incubation concentrations.

This quantification of ^{19}F per cell is necessary to calculate the amount of labeled cells required to visualize the fluorine signal with Magnetic Resonance Imaging (MRI).

Figure 6: ^{19}F Quantification of mOPCs using NMR Spectroscopy

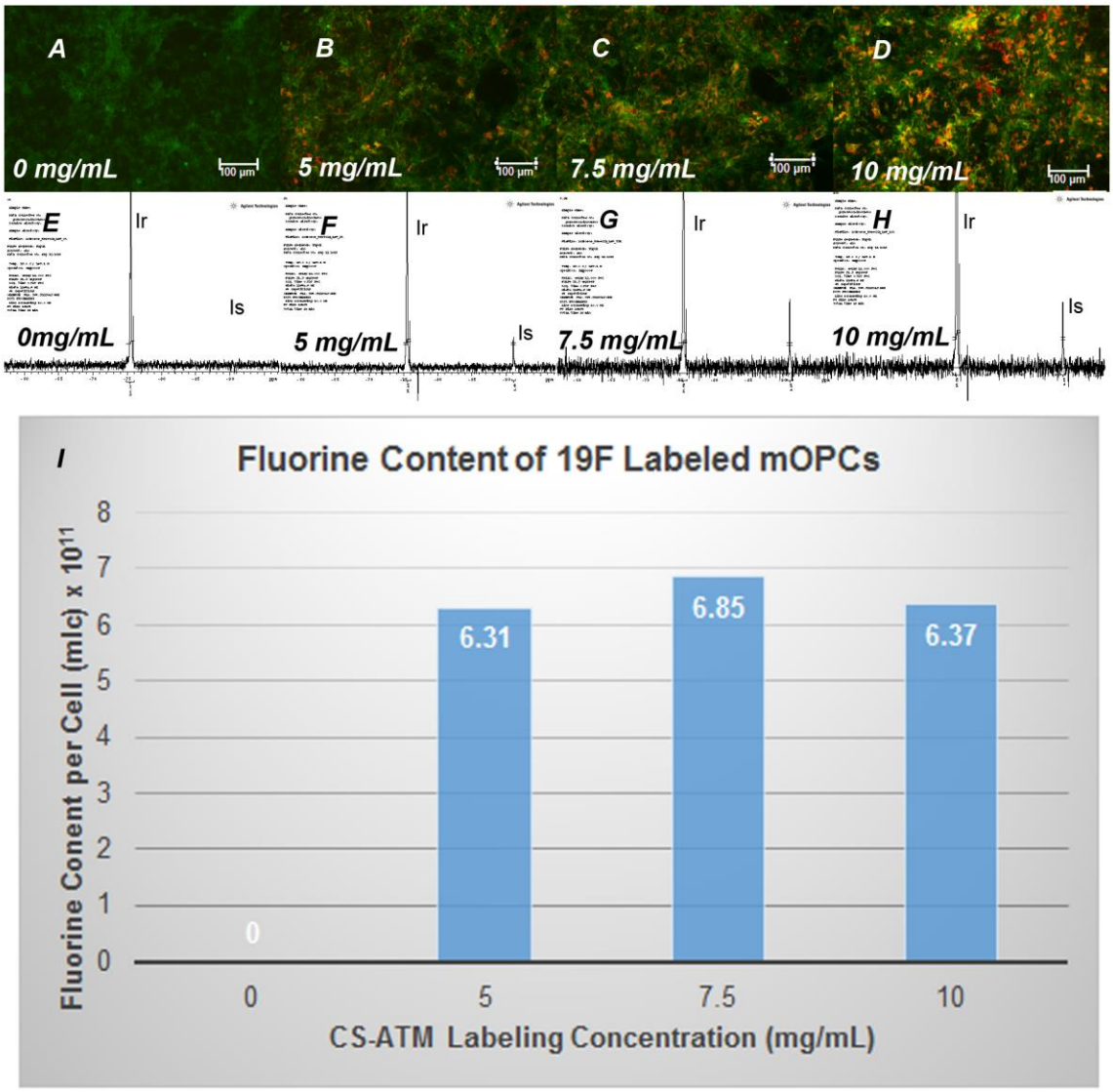

Figure 6: ^{19}F Quantification in mOPCs using NMR spectroscopy. (A-D) Fluorescent images were taken prior to harvesting for NMR to confirm fluorine uptake (red) in mOPCs expression transmembrane EGFP. Different labeling concentrations, 0 mg/mL (negative control) (A), 5 mg/mL (B), 7.5 mg/mL (C), and 10 mg/mL (D), of Cell Sense reagent are shown. Scale bars are 100 µm Corresponding NMR spectrums (E-H) for 0 mg/mL (E), 5 mg/mL (F), 7.5 mg/mL (G), and 10 mg/mL (H) labeling concentrations. On the spectrums, Ir designates the TFA reference peak at -91 ppm and Is designates the Cell Sense reagent peak at -76 ppm. The spectrums were used to calculate the amount of fluorine molecules per cell, shown in I. The X axis represents the labeling concentration, where the 3' indicates 3 mg/mL with 10% HSA and the Y axis is the amount of fluorine per cell. The numbers indicated on the graph are x10^{11}.

Table 2: Summary of NMR Spectroscopy Results

NMR Results				
Round 1	Concentration (mg/mL)	Ir	Is	^{19}F/cell (x10^{11})
100,000 cells	0	99.02	0.08	0.51
HLF	0'	99.1	0.1	0.32
	3	99.71	0.29	1.84
	3'	99.02	0.98	6.24
	5	99.94	1.06	6.7
Round 3				
80,000 - 100,000 cells	0	100	0	0
mOPC	0	100	0	0
	5	98.36	1.64	6.6
	5	98.5	1.5	6.02
	7.5	97.94	2.06	6.65
	7.5	97.82	2.18	7.05
	10	98.52	1.48	5.94
	10	98.31	1.69	6.8

Table 2: Summary of NMR spectroscopy Results. The NMR results for both the HLFs and mOPCs are listed here. In the first round of NMR, HLFs labeled with CS-ATM at 0 mg/mL, 3 mg/mL, 3 mg/mL + 10% HSA (designated as 3'), and 5 mg/mL. Each sample contained 100,000 cells. mOPCs were labeled with 0, 5, 7.5, and 10 mg/mL CS-ATM. All samples contained 80,000 cells, except for the 7.5 mg/mL samples with 100,000 cells. Ir represents the integrated area under the TFA reference peak and Is represents the integrated area of the major peak of the cell pellet for each sample. This information was used in the formula to calculate the number of fluorine atoms per cell (see methods), which is recorded in the column ^{19}F/cell. The values in this column are x10^{11}.

Labeling human iPSC-derived OPCs using 19F

hiPSC derived OPCs were also labeled using CS-ATM. hOPCs were incubated with 4 mg/mL CS-ATM diluted in hOPC media for 24 hours. HAS was not used in the ^{19}F culture, but is an area of future interest. After incubation and washing, the cells were fixed and fluorine uptake was confirmed with fluorescence microscopy (Figure 7B-D). No difference in cell morphology

was identified by microscopy between labeled cells and unlabeled control hOPCs. Further investigation is required to identify the optimal labeling concentration and cell viability after labeling for this cell population, including RFU analysis and NMR spectroscopy.

Figure 7: CS-ATM Labeled Human iPS cell derived OPCs.

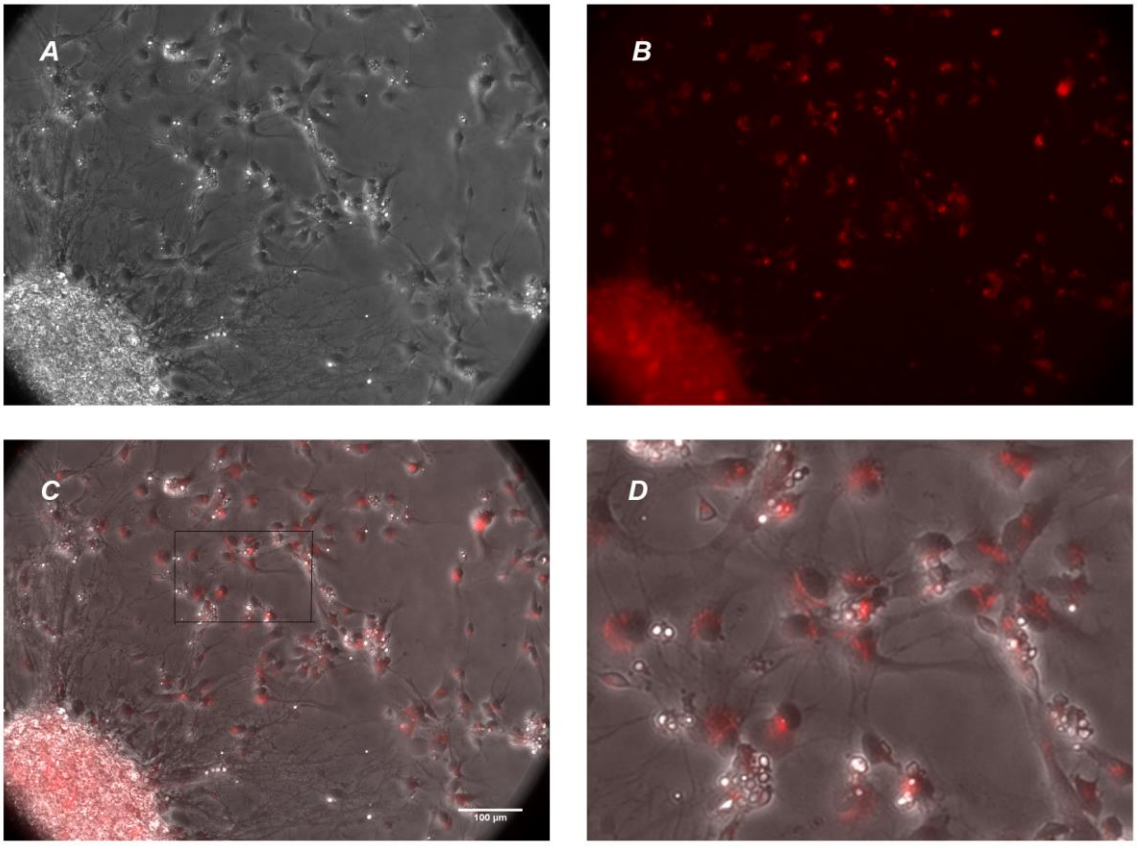

Figure 7: CS-ATM Labeled Human iPS cell derived OPCs. (A-D) hOPCs labeled with 4 mg/mL CS-ATM. Fluorescent images overlaid with phase to confirm uptake of fluorine. A-C are the same field taken at 20x of phase (A), red (B), and overlay (C). D shows a closer view of the overlaid image indicated by the black box on (C). 100 µm scale bar.

Magnetic Resonance Imaging of ^{19}Fluorine

The purpose of labeling cells with ^{19}F is to visualize fluorine labeled cells using MRI technology. To accomplish this, a custom made, dual-tone coil was generated by the University of Minnesota Center for Magnetic Resonance Research (CMRR) to detect ^{19}F signals. This can be used in combination with the proton signals generated from the Varian 16.4 T MRI scanner to create an overlaid image allowing visualization of the fluorine signal in cell or tissue context. The fluorine image would reveal cell "hotspots" on the proton image, allowing visualization of where the cells are located within the imaged tissue. This method would enable the CS-ATM compound to be used for tracking labeled cells after transplantation.

^{19}F detection by MRI in cell-free experiments

Two cell-free "phantom" experiments were used to examine the feasibility of imaging this fluorine reagent *in vivo* and to determine the optimal imaging configuration and settings.

The first phantom experiment used a relatively high concentration of CS-ATM (6 mg/mL, 1.55×10^{19} fluorine molecules) per sample arranged in our holding device (Figure 8A) to measure the homogeneity of the magnetic field inside the coil and magnet. Each of the 6 samples were visualized with minimal differences in pixel intensity, indicating a constant magnetic field within the imaging platform (data not shown). A consistent magnetic field is important to obtain accurate images; inconsistencies in the magnetic field can result in differences in detected fluorine signal intensities that are not indicative of differences in fluorine concentration.

A second cell-free "phantom" of CS-ATM was used to determine the minimum amount of ^{19}F molecules needed to produce a detectable signal with a high signal to noise ratio with MRI. The amount of fluorine molecules per tube were calculated and used based on physiological relevance. Six tubes were imaged, 5 tubes containing 1.55×10^{19}, 7.75×10^{18}, 1.55×10^{18}, 7.75×10^{17}, and 1.55×10^{17} fluorine molecules and 1 tube without ^{19}F (Figure 8C). Of the 5 tubes containing

CS-ATM, 4 could be seen (Figure 8B). The signal from tubes designated 2 and 3 was weakly detected, however the ^{19}F amounts in these samples were able to produce a signal strong enough to differentiate the signal from the background noise. The image was adjusted to optimize visualization of tube 4. The results of this image indicated the lower limit for ^{19}F detection to be between 1.55×10^{17} and 7.75×10^{18} ^{19}F molecules per 0.2 mL tube.

Figure 8: Cell-Free Phantom MRI Experiments

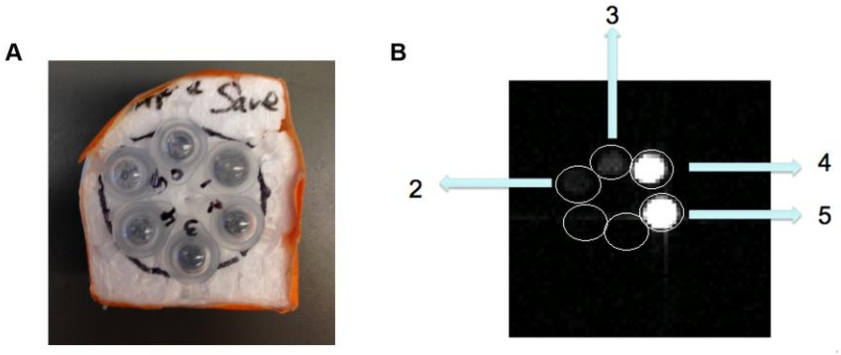

C

Tube	^{19}Fluorine Concentration
0	0
1	1.55×10^{17}
2	7.75×10^{17}
3	1.55×10^{18}
4	7.75×10^{18}
5	1.55×10^{19}

Figure 8: Cell-Free Phantom MRI Experiments. (A) A custom made apparatus was designed to hold 6 samples within a 2 cm diameter. The image obtained for the dose response of CS-ATM reagent alone is shown in B. Circles are drawn around the location of all 6 images, with 1 in the counter clock wise position next to 2, and 0 in between 1 and 6. (D) A table containing the fluorine concentrations is provided.

MRI detection of ^{19}F labeled cells

The third phantom experiment was designed to validate ^{19}F signal detection in CS-ATM cells and determine the required number of cells to generate a detectable image. The results from this phantom can be used to calculate the number of cells required per voxel to produce a detectable ^{19}F signal. The number of cells used in this experiment were based on the results from the second MRI phantom and the average concentration of ^{19}F per cell labeled with 5 mg/mL CS-ATM reagent detected by NMR analysis (6.3×10^{11} ^{19}F molecules per cell) (Table 2).

From our calculations, it was predicted the sample containing the highest number of cells would produce a signal with an intensity similar to the control sample containing the same amount of fluorine without cells, with each subsequent sample providing signals decreasing in intensity. However, following MRI analysis, the amount of fluorine in each tube and the positive control were insufficient to generate a visible signal against the background noise.

The MRI results confirm that under our conditions, the CS-ATM reagent can be visualized using MR technologies, however the labeling efficiency with mOPCs will require a higher cell concentration for appropriate signal intensity to create an optimal image. A combination of improvements could be utilized to generate a strong ^{19}F signal *in vivo*, including increased transplanted cell numbers, longer scan times, and optimization of the dual-tone coil to increase sensitivity. The 0.2 mL PCR sample tubes in the phantom experiments were used because of appropriate size and non-reactivity with the dual-tone coil, and to provide a sample of similar area size to that of a rat spinal cord analyzed after cell transplantation.

Table 3: Cell Number and Fluorine Concentration for Cell Phantom MRI Experiment.

Sample	Number of Cells	Fluorine Content
0	0	0
1	300,000	$2x10^{17}$
2	600,000	$4x10^{17}$
3	1,000,000	$6x10^{17}$
4	1,300,000	$8x10^{17}$
5	0	$7.75x10^{17}$

Table 3: Cell Number and Fluorine Concentration for Cell Phantom MRI Experiment. For each sample number, the corresponding cell number and fluorine content per tube are listed. Samples 0 and 5 represent the negative and positive controls, with no cells or fluorine and CS-ATM ^{19}F only, respectively.

Part B: Characterization of Transplanted Oligodendrocyte Progenitor Cells in the Injured Rat Spinal Cord

Short term experiments were conducted transplanting iPSC derived OPCs into rat spinal cords following contusion injury as described in the methods section; 20 age-matched rats were injured and received cell transplants 9 days later. Two of the rats were used as control animals, 8 rats received mOPCs, and 10 rats received hOPCs. One of the rats receiving hOPCs died shortly after the injection procedure, and the rest were sacrificed according to the timeline described (Figure 9). The purpose of this short term experiment is to determine if the transplanted iPS cell derived OPCs survive in the rat spinal cord after injection and to further characterize the transplanted cells after *in vivo* differentiation. This aspect of our study does not focus on functional improvement after cell transplantation in this model of spinal cord injury.

Figure 9: Short Term Rat Experimental Timeline

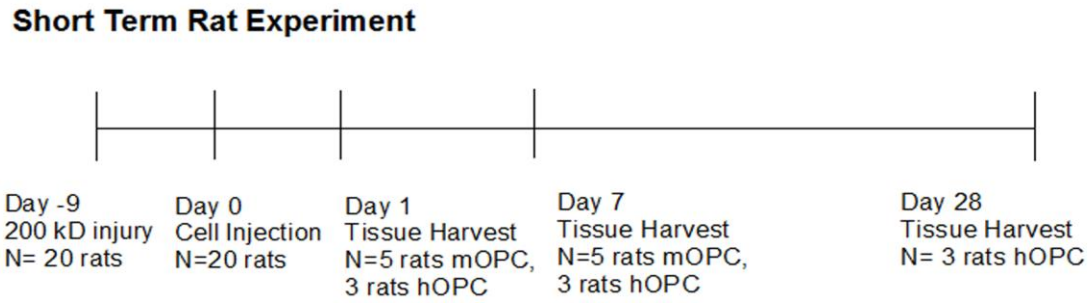

Figure 9: Short Term Rat Experimental Timeline. The rats receive contusion injuries 9 days before iPSC derived OPC transplants. Spinal cord tissues are harvested at 1 day, 1 week, and 1 month (28 days).

Histological Analysis of Spinal Cords Receiving mIPSC derived OPCS

The mOPCs used in this study express transmembrane bound eGFP. This allows for identification of transplanted cells by fluorescence microscopy. The majority of sections from injured rat spinal cords receiving miPS cell derived OPC transplants were found to contain eGFP expressing cells (Figure 10).

Figure 10: miPSC derived OPCs in the Injured Rat Spinal Cord

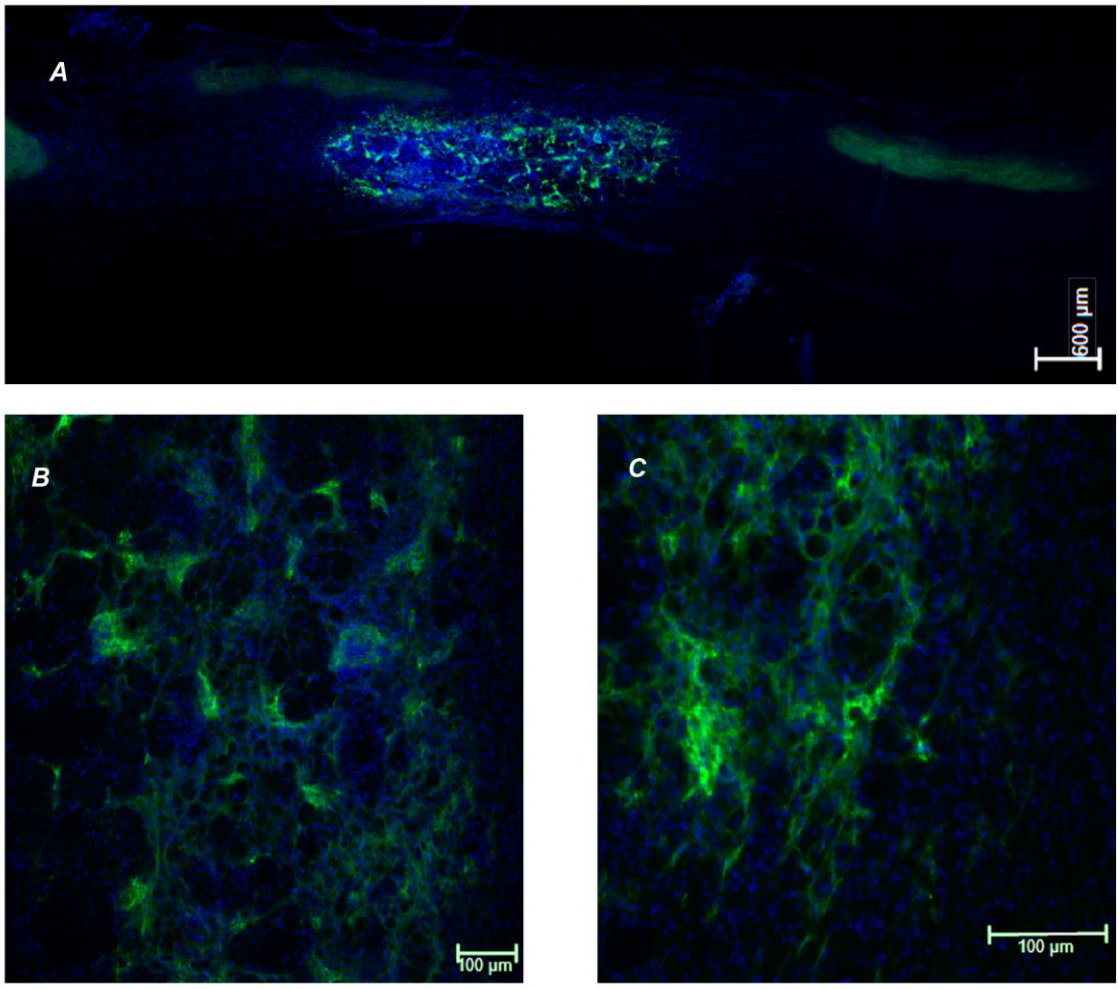

Figure 10: miPSC derived OPCs in the injured Rat Spinal Cord 1 week after transplantation. (A) A single parasagittal section containing eGFP expressing mOPCs merged with Dapi (blue). The dorsal and ventral sides of the spinal cord are the top and bottom, respectively. Scale bar 600 µm. A closer view of eGFP cells merged with Dapi in the rat spinal cord at 10x (B) and 20x (C). Scale bars 100 µm.

Characterization of Transplanted mOPCs with Immunohistochemistry

By one week after injection, the mOPCs have integrated into the tissue and have processes that are distant from the cell body and nucleus (Figure 10 B-D). This is a typical characteristic of OPCs becoming oligodendrocytes, creating projections that span and align with

neuronal axons to produce the protective myelin sheath. The projections seen confirm that the transplanted cells adopt the appropriate morphology of the oligodendrocyte lineage.

Further characterization of the transplanted mOPCs is ongoing, primarily through IHC. The antibodies that are being investigated include markers of OPCs and the oligodendrocyte lineage, Olig2, APC, MPB; cell division, Ki67; neurons, NF200, βIII Tubulin; and astrocytes, GFAP (Table 3). Olig2 (Oligodendrocyte lineage transcription factor 2) and APC (Adenomatous Polyposis Coli) are transcription factors expressed in the nucleus of cells in the oligodendrocyte lineage. Expression of these transcription factors in eGFP expressing cells confirms that the transplanted cells remained in the oligodendrocyte lineage and did not adopt another cell fate[45]. Myelin Basic Protein (MBP) is the major component of the myelin sheath, and can be seen in myelinating oligodendrocytes. The neuronal markers neurofilament (NF200) and βIII Tubulin have two functions; one to confirm that the transplanted mOPCs do not become neurons after injection, and two to visualize the interaction between the eGFP projections with the neuronal tracts. Finally, glial fibrillary acidic protein (GFAP) is used to show that the majority of transplanted cells do not adapt an astroglial fate.

Immunohistochemistry of Oligodendrocyte Markers

The majority of the markers have been analyzed in relation to the transplanted mOPCs, however the entirety of the cords have not been processed and quantification has not been completed. In most areas of dense eGFP expression, there is increased Olig2 expression compared to what is found in the endogenous spinal cord (Figure 11). Further analysis with confocal microscopy is required to definitively identify the nuclei corresponding to the eGFP transplanted cells. Additionally, APC expression was found near areas of eGFP expression (Figure 12A-B). APC indicates later-stage OPCs as they are differentiating into oligodendrocytes, thus a large percentage of APC expression mOPCs is not expected after 1 week in the spinal cord.

In culture, mOPCs are relatively proliferative when maintained in mOPC media. However, it is expected that after transplantation, the cells will be subjected to an environment promoting differentiation compared to proliferation. Ki67 staining has supported this hypothesis with a small fraction of the transplanted cells positive for Ki67, while the majority of mOPCs are negative. Figure 12C and D illustrate one area of Ki67 positive nuclei near a patch of eGFP expressing cells.

Figure 11: Olig2 analysis of mOPCs in the Injured Rat Spinal Cord

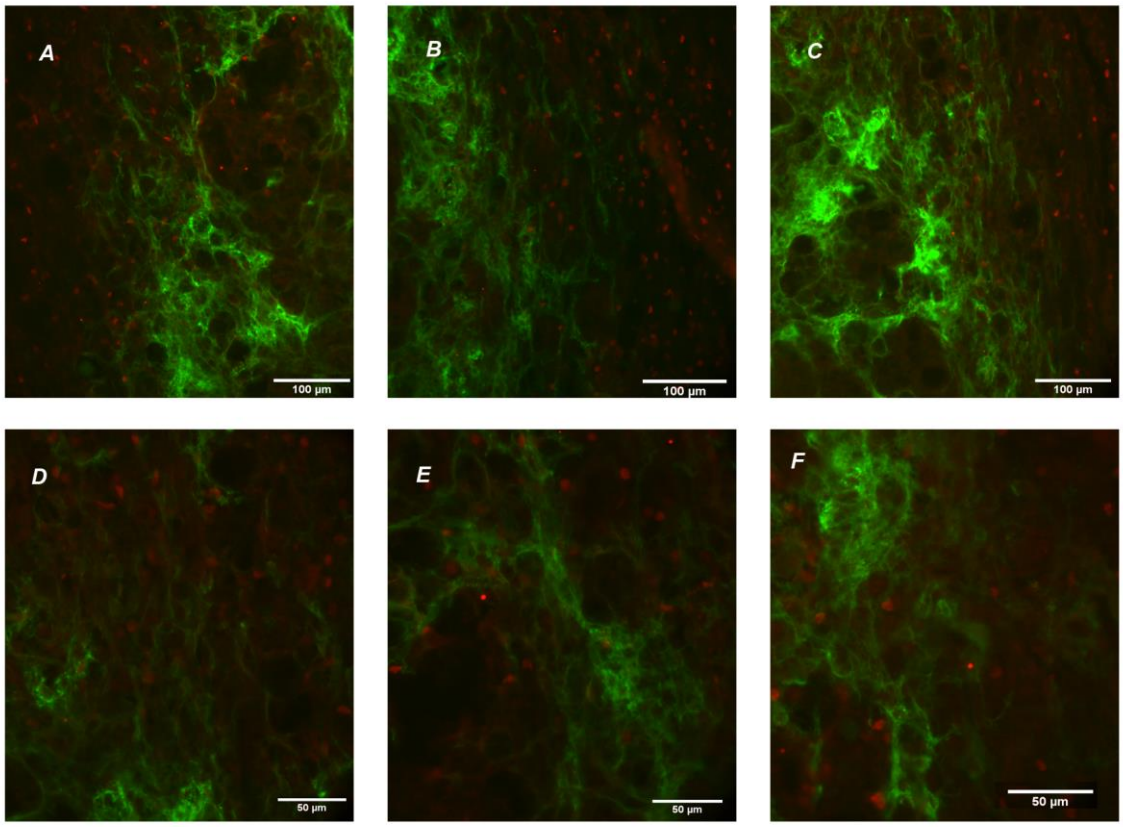

Figure 11: Olig2 Analysis of mOPCs in the Injured Rat Spinal Cord 1 week after transplantation. Fluorescent microscopy images of eGFP expressing cells with Olig 2 expression (Red) at 20x (A-C), and 40x (D-F).

Figure 12: APC and Ki67 Analysis of mOPCs in the Injured Rat Spinal Cord

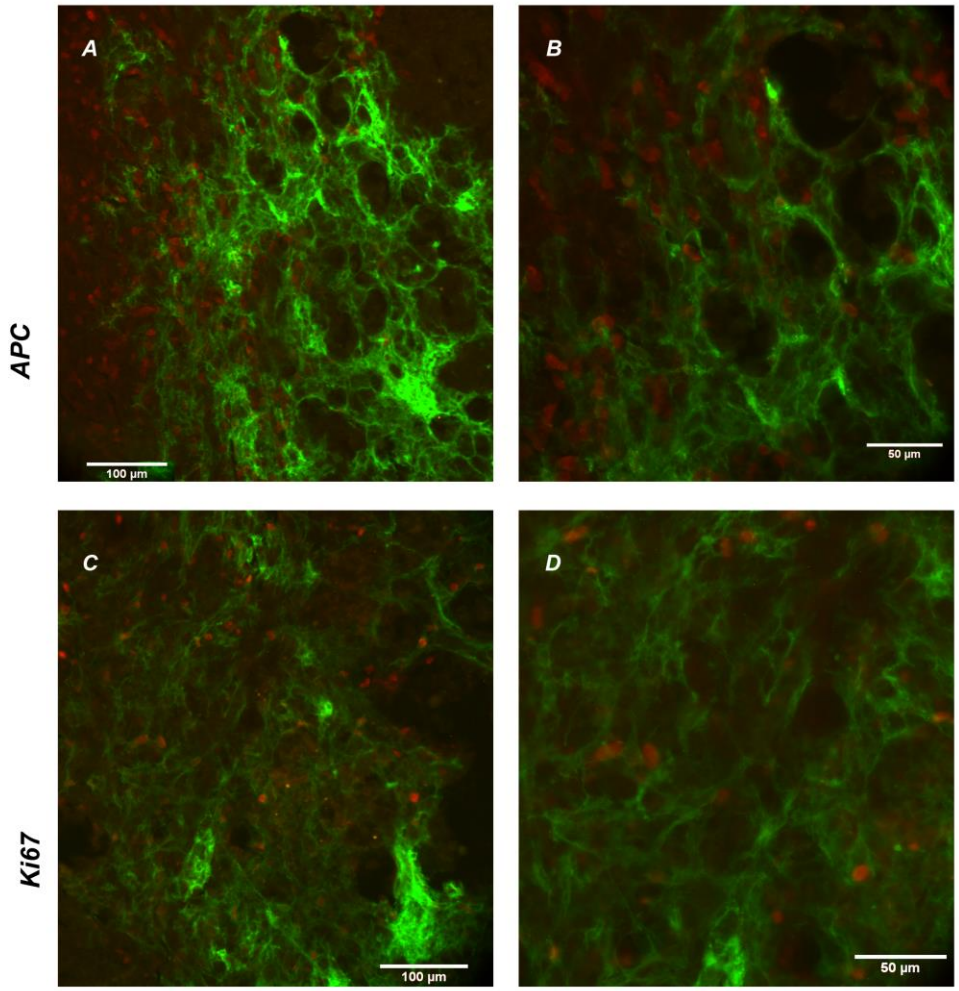

Figure 12: APC and Ki67 Analysis of mOPCs in the Injured Rat Spinal Cord 1 week after transplantation. Fluorescent microscopy images of eGFP expressing mOPCs with APC (Red) at 20x (A) and 40x (B) objectives. Example images of positive Ki67 (Red) at 20x (C) and 40x (D) objects are shown. Scale bars are 100 µm (A,C) and 50 µm (B,D).

Immunohistochemistry of Neuronal and Astroglial Markers

The neuronal markers NF200 and βIII Tubulin rarely overlap with the eGFP expressing mOPCs, confirming that the transplanted cells are not generating neurons. These markers show a

relationship between the eGFP mOPCs and neuronal tracts, as the eGFP projections appear to associate the neuronal tracts (Figure 13). Confocal microscopy will be utilized to further describe this relationship. Finally, a minimal amount, approximately less than 10% of the transplanted cells have become astrocytes, as indicated by GFAP staining (Figure 14).

Additionally, there is no evidence of tumor growth at the 1 day or 1 week time points. This is an important finding, providing evidence for the safety of transplanted mOPCs in an injured rat spinal cord.

Figure 13: Neurofilament and βIII Tubulin Analysis of mOPCs in the Injured Rat Spinal Cord

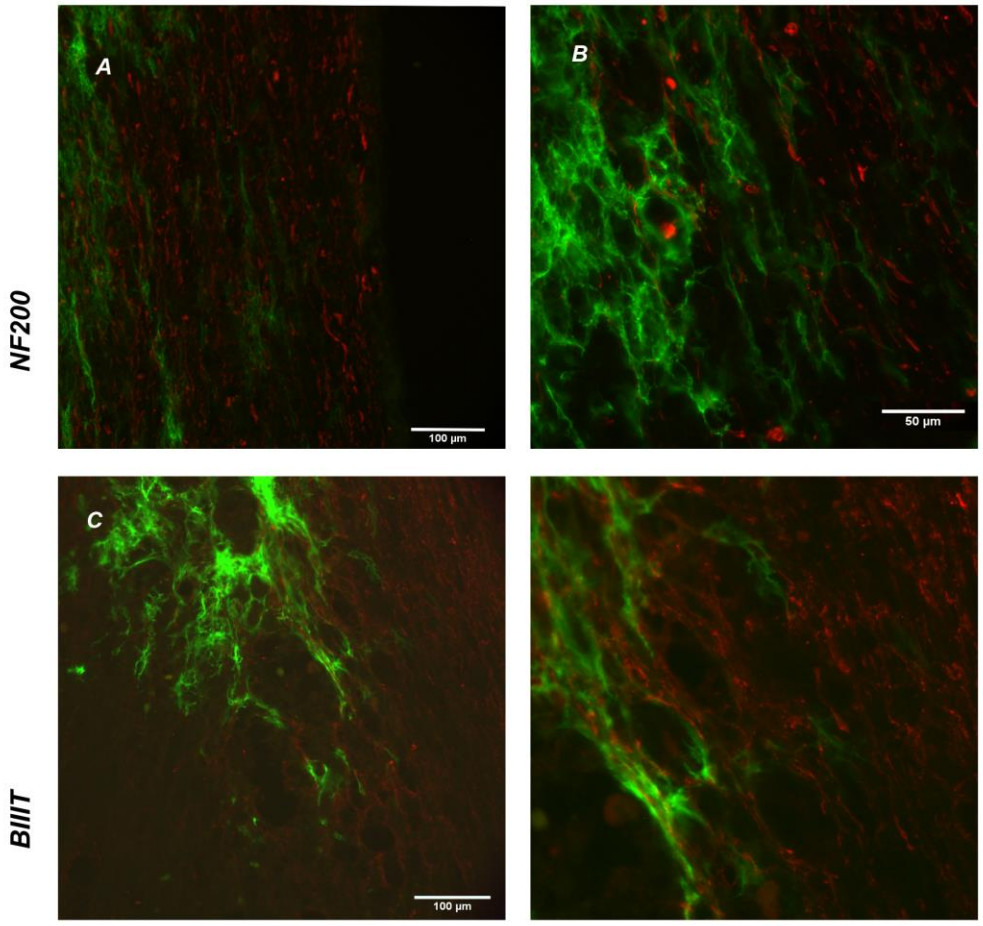

Figure 13: Neurofilament and βIII Tubulin Analysis of mOPCs in the Injured Rat Spinal Cord 1 week after transplantation. Fluorescent microscopy images of eGFP expressing mOPCs with neurofilament (NF200) (Red) at 20x (A) and 40x (B) objectives, and βIIITubulin (Red) at 20x (C) and 40x (D). Scale bars are 100 µm (A,C) and 50 µm (B.D).

Figure 14: GFAP Analysis of mOPCs in the Injured Rat Spinal Cord

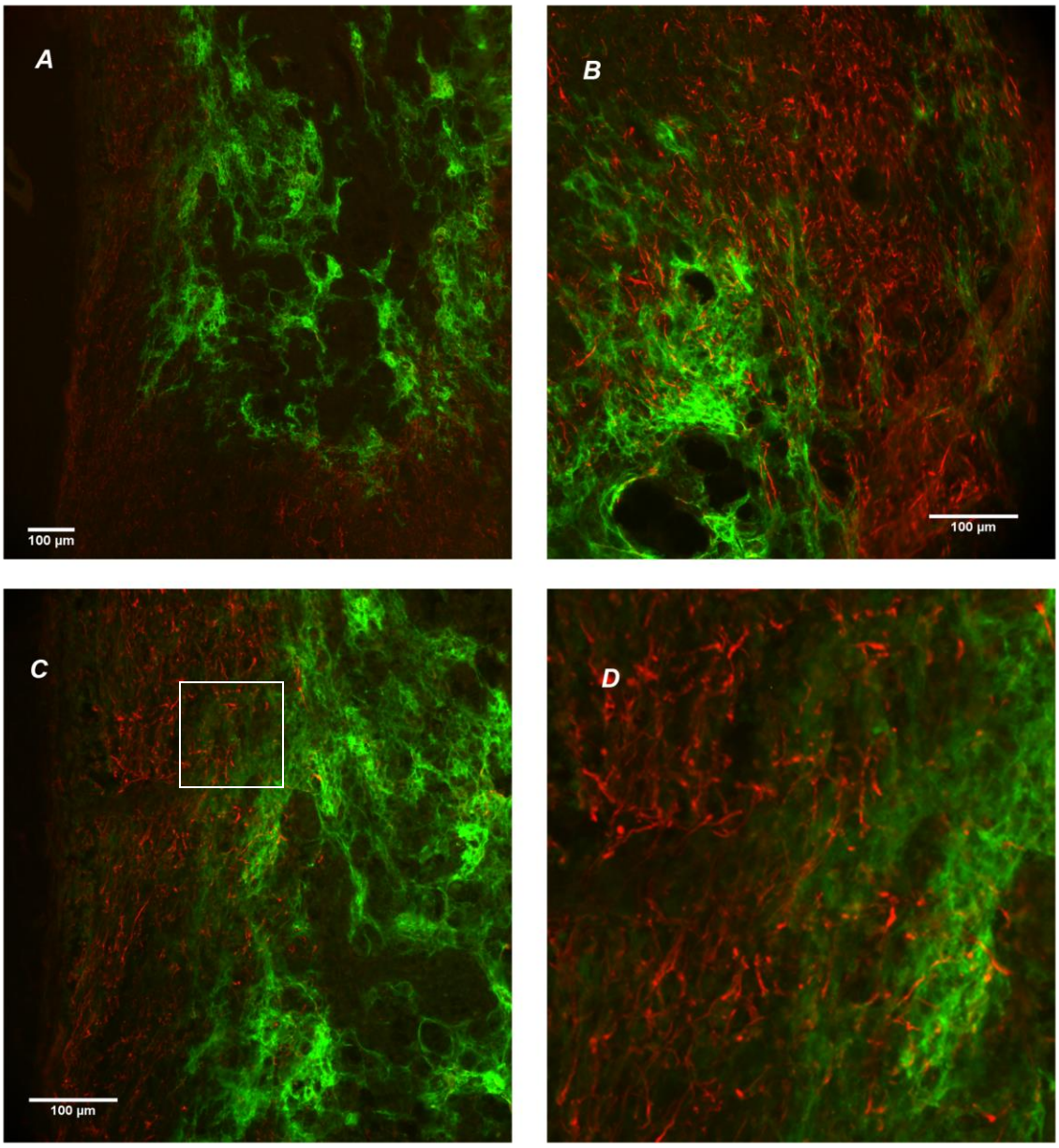

Figure 14: GFAP Analysis of mOPCs in the Injured Rat Spinal Cord 1 week after transplantation. Fluorescent microscopy images of eGFP expressing mOPCs with GFAP staining (Red) at 10x (A) and 20x (B and C). A zoomed in square of C is displayed in D, as indicated. Scale bars are 100 µm.

Characterization of transplanted hiPSC derived OPCs

The transplanted hOPCs in the short term rat experiment do not express a lineage tracer, such as eGFP, making tracking of the transplanted cells more challenging. The host and donor cells are from distinct species allowing for multiple techniques to distinguish the cells from each species. In this experiment, antibodies against human cells, SC121, a human cytoplasmic marker, is used to distinguish transplanted human cells from endogenous rat cells. The cytoplasmic marker, SC121, works well with minimal non-specific binding, labeling the majority of each human cell to show the morphology and projections (Figure 15, Figure 16).

Utilizing the SC121 antibody, the transplanted human cells can be seen after 1 day, 1 week (Figure 15), and 1 month (28 days) (Figure 16), providing evidence that transplanted human cells can survive in the rat spinal cord without the use of additional immunosuppression. This antibody has also shown that many of the human cells on the perimeter of the transplanted cells have obtain a morphology similar to oligodendrocytes, with long, thin processes (Figure 16).

Figure 15: hiPSC derived OPCs in the Injured Rat Spinal Cord 1 week after Transplantation

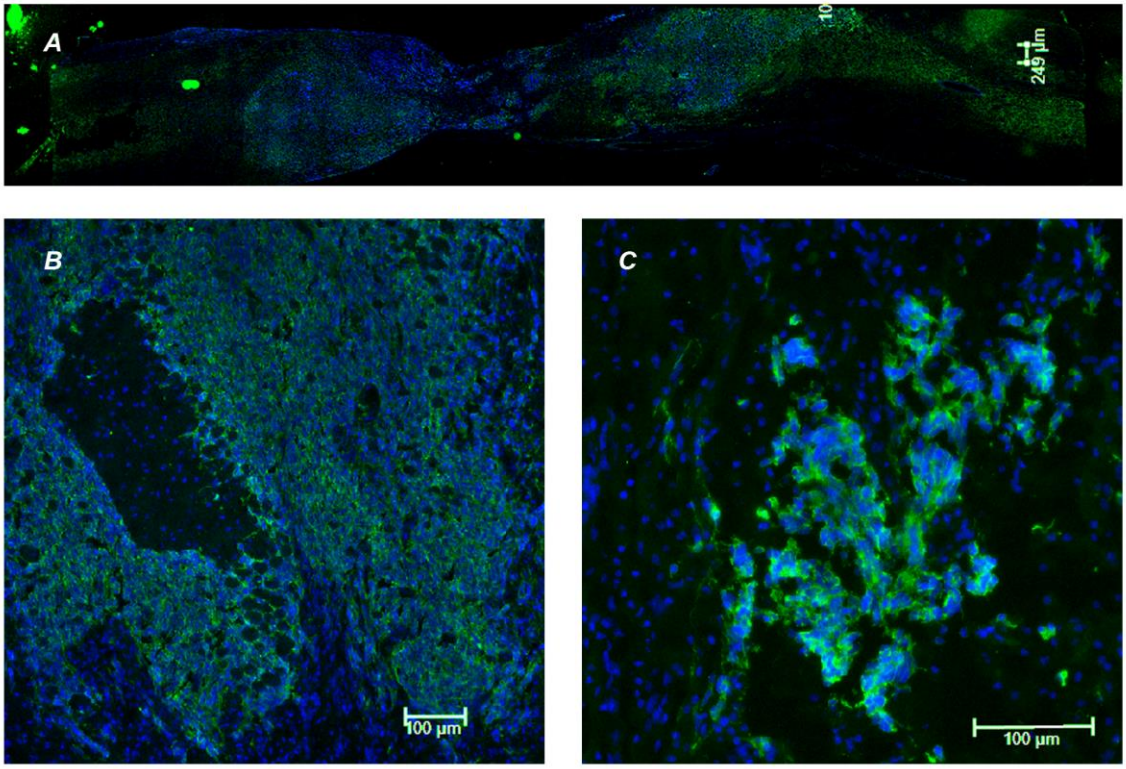

Figure 15: hiPSC derived OPCs 1 week after transplant to injured rat spinal cord. (A) A tiled image of a single, parasagittal rat spinal cord section containing SC121 positive human cells (green). Close up images at 10x (B) and 20x (C) objectives displaying human cells in the rat spinal cord with Dapi (blue). Scale bars are 250 µm (A) and 100 µm (B,C)

Figure 16: hiPSC derived OPCs in the Injured Rat Spinal Cord 1 Month after Transplantation

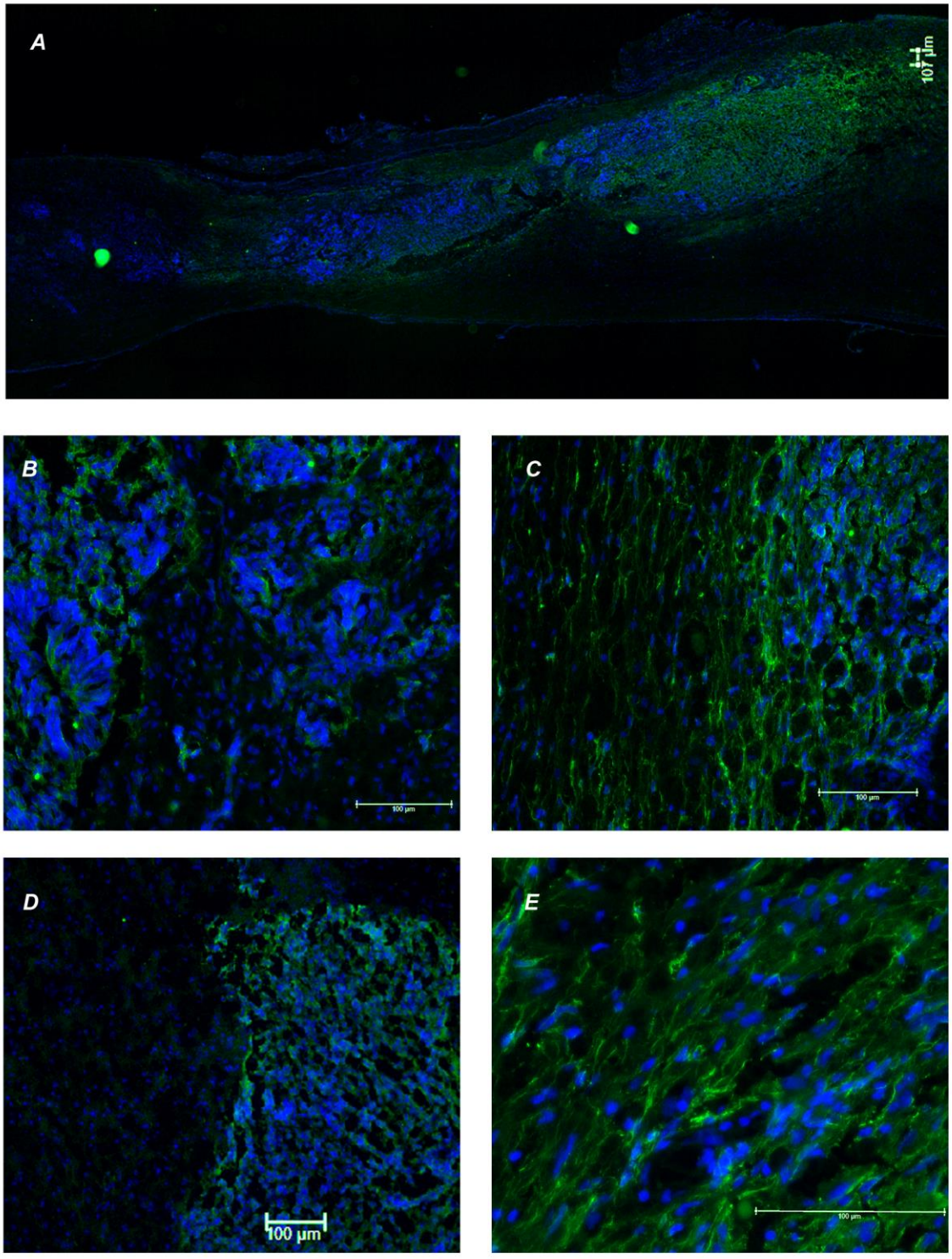

Figure 16: hiPSC derived OPCs in the Injured Rat Spinal Cord 1 month after transplantation. (A) A tiled image of a single, parasagittal rat spinal cord section containing SC121 positive human cells (green). Close up images at 20x (B and C), 10x (D), and 40x (E) objections displaying human cells in the rat spinal cord counterstained with Dapi (blue). Scale bars are 100 µm.

Characterization of the transplanted hiPSC derived OPCs is ongoing, however some of the initial staining has been completed. There appears to be overlap of SC121 with Olig2 expression, however further analysis with confocal and human nuclear antigen is required (Figure 17). Additionally, Ki67 staining shows that a small population of the transplanted hOPCs are dividing. Pax 6 expression was also analyzed to determine if the transplanted cells are generating neurons. A small subset of transplanted hOPCs are near patches of Pax 6 expression. However, the majority of hOPCs appear to remain in the oligodendrocyte lineage. Further analysis of these transplanted cells is required for complete characterization. Overall these results demonstrate that the hiPSC derived OPCs can survive after transplantation into the injured rat spinal cord.

Figure 17: hiPSC derived OPCs Counterstained with Olig2 in the Injured Rat Spinal Cord

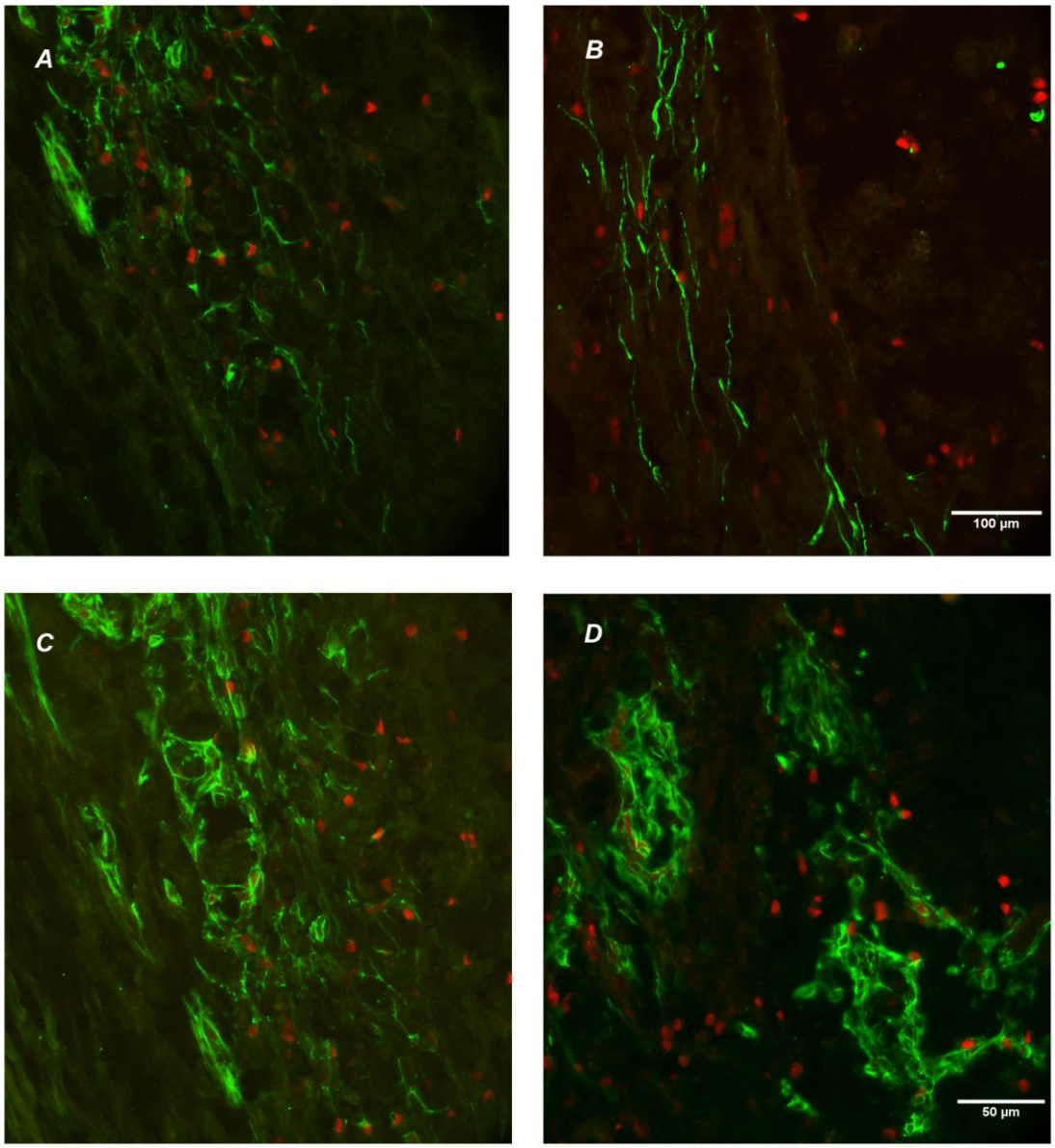

Figure 17: hiPSC derived OPCs Counterstained with Olig2 in the Injured Rat Spinal Cord. Rat spinal cords receiving hOPC transplants were stained for SC121 to label human cells (green) and counterstained with Olig2 (red). Fluorescent images taken at 20x (A and B), and 40x (C and D) objectives are shown. Scale bars are as 100 µm (A,B) and 50 µm (C,D).

Discussion

The purpose of this research was to validate the use of ^{19}fluorine labeling to track oligodendrocyte progenitor cells *in vivo* after transplantation into injured rat spinal cord and to characterize transplanted oligodendrocyte progenitor cells in injured rat spinal cords.

The results from *ex vivo* cell labeling with the ^{19}F Cell Sense reagent are consistent with published data, confirming low toxicity and minimal phenotypic effects after labeling. The use of HSA in the culture medium increased fluorine uptake by cells, supported by NMR analysis, similar to results found by Bible et al. (2012). In the HLF cell NMR analysis, the sample containing 3 mg/mL had fewer fluorine molecules per cell than the sample containing 3mg/mL with HSA. Some of this difference can be accounted for by the use of HSA to increase fluorine uptake *ex vivo*, however it is possible that mechanical error is also influencing this large difference in fluorine concentration. For instance, the 3 mg/mL sample may have had fewer cells than calculated or differences could have occurred in NMR processing. Overall, these *ex vivo* cell labeling findings are consistent with the literature and the manufacturer's findings, supported by accurate NMR quantification of fluorine content per cell. Further analysis of ^{19}F CS-ATM labeling in hiPSC derived OPCs is required to accurately quantify fluorine content after labeling and to identify the optimal labeling concentration with the greatest fluorine concentration per cell to cell death ratio. Replication of the results is necessary for further analysis.

Magnetic resonance imaging results validated that a ^{19}F signal can be detected with our coil, MRI scanner and instruments, however the amount of cells necessary to generate a signal at our labeling efficiency is greater than expected. It is possible to increase the cellular concentration within the 0.2 mL PCR tube to generate a signal with an intensity great enough to be visualized with our custom made ^{19}F coil. However, in the injured rat spinal cord, increasing the cell concentration above 1,500,000 transplanted cells would be impossible due to the physiological stress of transplanting such a large quantity of cell into soft tissue. This quantity of

cells is realistic for transplantation into injured human spinal cords, however the translation of resolution between imaging rats and humans is unclear. The next step will be to quantify the pixel intensity of the MR image and to calculate the number of cells required per voxel for ^{19}F signal detection.

Although visualization of mOPCs labeled with CS-ATM in an injured rat spinal cord is challenging, human iPSC derived OPCs may have a higher fluorine uptake efficiency, decreasing the amount of cells required to generate a ^{19}F image with MR technologies. Alternatively, it may be possible to transplant the appropriate number of labeled mOPCs required for imaging in a *shiverer* mouse brain. *Shiverer* mice have a genetic defect creating a large deletion in the myelin basic protein (MBP) gene, causing extensive dysmyelination in the CNS[46,47]. This model organism is utilized in our laboratory to test myelination by iPS cell derived OPCs. A larger quantity and volume of cells can be injected into these mice without causing fatal brain damage. With this model, the ^{19}F CS-ATM labeled cells can be visualized with MRI, and the quantification and migratory ability of OPCs can be assessed by imaging transplanted OPCs at different time points following transplantation. This study would also provide information regarding ^{19}F label retention and imaging following transplantation. Label retention is difficult to assess *ex vivo* due to the proliferative phenotype of OPCs in culture, with each cell division diluting the ^{19}F signal. Label dilution should not be a problem in transplanted cells as it is hypothesized that transplanted OPCs are subjected to a microenvironment that promotes differentiation rather than proliferation, however this needs to be confirmed. The ability to track transplanted cells in injured spinal cords would allow the relationship between improved function and retention of transplanted cells to be assessed. For instance, functional testing, *in vivo* cell tracking of labeled OPCs, and myelin imaging via MRI can be assessed for the same animal at different time points, providing more informative results of the progress in each animal individually.

The traditional method of tracking cells is to harvest tissue at specific time points after transplantation and identify the transplanted cells through histological analysis, primarily immunohistochemistry (IHC). The use of *in vivo* cell tracking with reagents such as CS-ATM allows researchers to track the transplanted cells in live animals. In early experiments with transplanted, CS-ATM labeled OPCs, it will be important to analyze the tissues at each time point after *in vivo* to confirm the MRI results.

Significant advantages of ^{19}Fluorine use for cell tracking in transplantation experiments exist, including non-toxicity, high resolution, ability to quantify cells, and potential to visualize the biodistribution of the transplanted cells. For safety studies it is important to determine if there is accumulation of the transplanted cells in other organs, such as the lungs, which can be detected with ^{19}F MRI. However, there are some pitfalls to this tracking approach. One obstacle is potential signal dilution after cell division. This may not affect imaging if the fluorine content in a specific area remains the same, but if the cell division significantly expands the area in which the fluorine molecules are present, the signal intensity will decrease. This result could potentially affect cell counts based on fluorine signal, however appropriate controls to identify the amount of cell division after transplantation would help estimate this occurrence. Additionally, there is potential for false positives. If death of transplanted, labeled cells occurs, it is possible that macrophages or phagocytes in the surrounding area may obtain the ^{19}F molecules through cell debris. This is a potentially significant problem in the spinal cord after injury as there is infiltration of macrophages. To account for this in initial experiments, corresponding analysis of the transplanted, injured rat spinal cord using IHC for phagocyte markers would indicate the amount of overlap between the red, ^{19}F signal and any phagocytic cells.

Characterization of OPCs transplanted into the injured rat spinal cords with CS-ATM labeling is currently underway. Immunohistochemistry results have confirmed that we can detect our transplanted OPCs, both mouse and human, in frozen sections of the rat spinal cord. Further

analysis, primarily with confocal microscopy is required to confirm co-expression of transplanted cells with OPC and oligodendrocyte markers.

The next step in characterization is quantification of transplanted OPCs. Due to the transmembrane expression of eGFP, the mOPCs are difficult to quantify given the extensive eGFP expressing processes. It is difficult to determine which nuclei corresponds to each eGFP cell body. The human SC121 cytoplasmic staining also provides this challenge, however quantification of human cells may be accomplished with human nuclear antigen staining. The human nuclear antigen provides a solution to total transplanted cell quantification and calculation of the percent of transplanted cells co-expressing OPC nuclear markers, however the cytoplasmic marker (SC121) is more informative for counterstaining for structural proteins, such as GFAP, neurofilament, and MBP.

Of the characterization completed, IHC results indicate that the transplanted OPCs and their progeny are retained, with few transplanted cells generating neurons or astrocytes.

Overall, the results of this thesis confirm that the ^{19}F Cell Sense reagent is feasible because of low toxicity for use in both mouse and human OPCs, with similar labeling efficiencies to other studies and cell types. The MRI technologies available are sufficient to visualize a strong ^{19}F signal, however a more sensitive dual-tone coil may be required to detect the ^{19}F signal in CS-ATM labeled OPCs.

Histological analysis of transplanted OPCs into injured rat spinal cords can be accurately assessed based on the parameters determined in this research. In the future, labeled OPCs can be transplanted into injured spinal cords and tracked *in vivo*, as well as characterized by IHC. The use of the research ^{19}F with the red fluorescent dye would also help to identify transplanted hOPCs prior to staining. This would not only allow for tracking via MR imaging but also using fluorescence microscopy visualizing the red fluorescent dye in transplanted cells. The *in vivo*

analysis will not only allow us to track the migration of transplanted cells, but also quantify the number of surviving cells and link this to functional improvements after transplant.

The use of this FDA approved ^{19}F reagent can be potentially translated directly to human use. Future clinical trials investigating cell therapies in patients with chronic spinal cord injury would greatly benefit from this *in vivo* ^{19}F cell tracking method to further assess safety and efficacy of transplanted OPCs, both through the tracking and quantification analysis that can be pursued with CS-ATM.

Bibliography

1. Crawford, a H., Chambers, C. & Franklin, R. J. M. Remyelination: the true regeneration of the central nervous system. *J. Comp. Pathol.* **149,** 242–54 (2013).

2. Felts, P. A., Baker, T. A. & Smith, K. J. Conduction in Segmentally Demyelinated Mammalian Central Axons. *J. Neurosci.* **17,** 7267–7277 (1997).

3. Kessaris, N. *et al.* Competing waves of oligodendrocytes in the forebrain and postnatal elimination of an embryonic lineage. *Nat. Neurosci.* **9,** 173–9 (2006).

4. Bradl, M. & Lassmann, H. Oligodendrocytes: biology and pathology. *Acta Neuropathol.* **119,** 37–53 (2010).

5. Masahira, N. *et al.* Olig2-positive progenitors in the embryonic spinal cord give rise not only to motoneurons and oligodendrocytes, but also to a subset of astrocytes and ependymal cells. *Dev. Biol.* **293,** 358–69 (2006).

6. Noble, M., Pröschel, C. & Mayer-Pröschel, M. Getting a GR(i)P on oligodendrocyte development. *Dev. Biol.* **265,** 33–52 (2004).

7. Miller, R. H. Regulation of oligodendrocyte development in the vertebrate CNS. *Prog. Neurobiol.* **67,** 451–467 (2002).

8. Miron, V. E., Kuhlmann, T. & Antel, J. P. Cells of the oligodendroglial lineage, myelination, and remyelination. *Biochim. Biophys. Acta* **1812,** 184–93 (2011).

9. Alsanie, W. F., Niclis, J. C. & Petratos, S. Human embryonic stem cell-derived oligodendrocytes: protocols and perspectives. *Stem Cells Dev.* **22,** 2459–76 (2013).

10. Jiang, P., Selvaraj, V. & Deng, W. Differentiation of embryonic stem cells into oligodendrocyte precursors. *J. Vis. Exp.* (2010). doi:10.3791/1960

11. Keirstead, H. S. *et al.* Human embryonic stem cell-derived oligodendrocyte progenitor cell transplants remyelinate and restore locomotion after spinal cord injury. *J. Neurosci.* **25,** 4694–705 (2005).

12. Hu, B.-Y., Du, Z.-W., Li, X.-J., Ayala, M. & Zhang, S.-C. Human oligodendrocytes from embryonic stem cells: conserved SHH signaling networks and divergent FGF effects. *Development* **136,** 1443–52 (2009).

13. Sharp, J., Frame, J., Siegenthaler, M., Nistor, G. & Keirstead, H. S. Human embryonic stem cell-derived oligodendrocyte progenitor cell transplants improve recovery after cervical spinal cord injury. *Stem Cells* **28,** 152–63 (2010).

14. Pouya, A., Satarian, L., Kiani, S., Javan, M. & Baharvand, H. Human induced pluripotent stem cells differentiation into oligodendrocyte progenitors and transplantation in a rat model of optic chiasm demyelination. *PLoS One* **6,** e27925 (2011).

15. Li, Y. *et al.* Differentiation of oligodendrocyte progenitor cells from human embryonic stem cells on vitronectin-derived synthetic peptide acrylate surface. *Stem Cells Dev.* **22,** 1497–505 (2013).

16. Czepiel, M. *et al.* Differentiation of induced pluripotent stem cells into functional oligodendrocytes. *Glia* **59,** 882–92 (2011).

17. Wang, S. *et al.* Human iPSC-derived oligodendrocyte progenitor cells can myelinate and rescue a mouse model of congenital hypomyelination. *Cell Stem Cell* **12,** 252–64 (2013).

18. Douvaras, P. *et al.* Efficient generation of myelinating oligodendrocytes from primary progressive multiple sclerosis patients by induced pluripotent stem cells. *Stem cell reports* **3,** 250–9 (2014).

19. Hagg, T. & Oudega, M. Degenerative and spontaneous regenerative processes after spinal cord injury. *J. Neurotrauma* **23,** 264–80 (2006).

20. Ankeny, D. P. & Popovich, P. G. Mechanisms and implications of adaptive immune responses after traumatic spinal cord injury. *Neuroscience* **158,** 1112–21 (2009).

21. Horky, L. L., Galimi, F., Gage, F. H. & Horner, P. J. Fate of endogenous stem/progenitor cells following spinal cord injury. *J. Comp. Neurol.* **498,** 525–38 (2006).

22. Faulkner, J. & Keirstead, H. S. Human embryonic stem cell-derived oligodendrocyte progenitors for the treatment of spinal cord injury. *Transpl. Immunol.* **15,** 131–42 (2005).

23. Nistor, G. I., Totoiu, M. O., Haque, N., Carpenter, M. K. & Keirstead, H. S. Human embryonic stem cells differentiate into oligodendrocytes in high purity and myelinate after spinal cord transplantation. *Glia* **49,** 385–96 (2005).

24. Xiao, L., Saiki, C. & Ide, R. Stem cell therapy for central nerve system injuries: glial cells hold the key. *Neural Regen. Res.* **9,** 1253–60 (2014).

25. Mothe, A. J. & Tator, C. H. Advances in stem cell therapy for spinal cord injury. *J. Clin. Invest.* **122,** 3824–34 (2012).

26. Piltti, K. M., Salazar, D. L., Uchida, N., Cummings, B. J. & Anderson, A. J. Safety of human neural stem cell transplantation in chronic spinal cord injury. *Stem Cells Transl. Med.* **2,** 961–74 (2013).

27. Bartusik, D. & Aebisher, D. (19)F applications in drug development and imaging - a review. *Biomed. Pharmacother.* **68,** 813–817 (2014).

28. Chen, H., Viel, S., Ziarelli, F. & Peng, L. 19F NMR: a valuable tool for studying biological events. *Chem. Soc. Rev.* **42,** 7971–82 (2013).

29. Ahrens, E. T. & Zhong, J. In vivo MRI cell tracking using perfluorocarbon probes and fluorine-19 detection. *NMR Biomed.* **26,** 860–71 (2013).

30. Krafft, M. Emulsions and microemulsions with a fluorocarbon phase. *Curr. Opin. Colloid Interface Sci.* **8,** 251–258 (2003).

31. Berger, A. Magnetic resonance imaging. *BMJ* **324,** 35 (2002).

32. Hwang, Y. H. & Lee, D. Y. Magnetic resonance imaging using heparin-coated superparamagnetic iron oxide nanoparticles for cell tracking in vivo. *Quant. Imaging Med. Surg.* **2,** 118–23 (2012).

33. Sykova, E. & Jendelova, P. In vivo tracking of stem cells in brain and spinal cord injury. *Prog. Brain Res.* **161,** 367–83 (2007).

34. Bible, E. *et al.* Non-invasive imaging of transplanted human neural stem cells and ECM scaffold remodeling in the stroke-damaged rat brain by 19 F-and diffusion-MRI. *Biomaterials* **33,** 2858–2871 (2012).

35. Ahrens, E. & Helfer, B. Clinical cell therapy imaging using a perfluorocarbon tracer and fluorine-19 MRI. *Magn. Reson. …* **00,** (2014).

36. Ahrens, E. T., Flores, R., Xu, H. & Morel, P. a. In vivo imaging platform for tracking immunotherapeutic cells. *Nat. Biotechnol.* **23,** 983–7 (2005).

37. Srinivas, M., Boehm-Sturm, P., Figdor, C. G., de Vries, I. J. & Hoehn, M. Labeling cells for in vivo tracking using (19)F MRI. *Biomaterials* **33,** 8830–40 (2012).

38. Janjic, J. M., Srinivas, M., Kadayakkara, D. K. K. & Ahrens, E. T. Self-delivering Nanoemulsions for Dual Fluorine-19 MRI and Fluorescence Detection. 2832–2841 (2008).

39. Helfer, B. M. *et al.* Functional assessment of human dendritic cells labeled for in vivo (19)F magnetic resonance imaging cell tracking. *Cytotherapy* **12,** 238–50 (2010).

40. Boehm-Sturm, P., Mengler, L., Wecker, S., Hoehn, M. & Kallur, T. In vivo tracking of human neural stem cells with 19F magnetic resonance imaging. *PLoS One* **6,** e29040 (2011).

41. Ribot, E. J., Gaudet, J. M., Chen, Y., Gilbert, K. M. & Foster, P. J. In vivo MR detection of fluorine-labeled human MSC using the bSSFP sequence. *Int. J. Nanomedicine* **9,** 1731–1739 (2014).

42. Srinivas, M., Morel, P. a, Ernst, L. a, Laidlaw, D. H. & Ahrens, E. T. Fluorine-19 MRI for visualization and quantification of cell migration in a diabetes model. *Magn. Reson. Med.* **58,** 725–34 (2007).

43. Boehm-Sturm, P. *et al.* A multi-modality platform to image stem cell graft survival in the naïve and stroke-damaged mouse brain. *Biomaterials* **35,** 2218–26 (2014).

44. Greder, L. V. *et al.* Brief report: Analysis of endogenous Oct4 activation during induced pluripotent stem cell reprogramming using an inducible Oct4 lineage label. *Stem Cells* **30,** 2596–2601 (2012).

45. Lang, J. *et al.* Adenomatous polyposis coli regulates oligodendroglial development. *J. Neurosci.* **33,** 3113–30 (2013).

46. Bin, J. M., Leong, S. Y., Bull, S.-J., Antel, J. P. & Kennedy, T. E. Oligodendrocyte precursor cell transplantation into organotypic cerebellar shiverer slices: a model to study myelination and myelin maintenance. *PLoS One* **7,** e41237 (2012).

47. Duncan, I. D., Kondo, Y. & Zhang, S.-C. The myelin mutants as models to study myelin repair in the leukodystrophies. *Neurotherapeutics* **8,** 607–24 (2011).